

Hydraulic characterization of a part of the Rietholzbach area

Master Thesis

Geo 511

Cornelia Wigger
S09752338

Supervisor: Dr.-Ing. Dirk Radny
Dirk.Radny@eawag.ch

Professor: Jan Seibert

Universität Zürich in cooperation with Eawag

Mathematisch-naturwissenschaftliche Fakultät
Geographisches Institut
Physische Geographie
Hydrologie und Klima (H2K)

Aquatic Research Institut
Wasserressourcen + Trinkwasser
Hydrogeologie
8600 Dübendorf

6th November 2013

Zürich, 2013

Abstract

Floods are part of the history of rivers and their landscape. Due to precipitation and snow melt the system is replenished and saturated sometime. Hence, a faster and larger overland flow occurs and floods emerge. Especially the Thur river, which has no retention basin, reacts fast and dynamically of floods. Thus it is of major importance to have detailed knowledge about the hydraulic processes in the Thur catchment, located in the north-eastern part of Switzerland. Hence, this thesis investigates runoff components of a pre-alpine slope in the Rietholzbach area, which is a tributary of the Thur river. In this thesis, precipitation, infiltration, overland flow, baseflow and stream flow are the processes, that were investigated by double-ring infiltration measurements, slug-out tests and salt tracer tests. Based on past research results this study gives an overview about the hydraulic characterization of a part of the Rietholzbach area. Resulting from this investigation the infiltration rate decreases top down and so does the hydraulic conductivity of the subsurface. Additionally, an interaction between ground water and stream flow, in form of baseflow was detected. The discharge of the Rietholzbach increases by passing through the investigated area in an empty as well as in a full system, due to the permanent inflow from the ground water.

Contents

1	Introduction	4
2	Fundamental Principles	6
2.1	Site Description	6
2.1.1	Location	6
2.1.2	Geology	8
2.1.3	Soil	9
2.1.4	Climatology	10
2.1.5	Land Use	11
2.2	Theoretical Background	11
2.2.1	Overland Flow	12
2.2.2	Interflow	12
2.2.3	Baseflow	13
2.2.4	Stream Flow	13
2.2.5	Infiltration	14
2.2.6	Hydraulic conductivity	14
3	Methods	16
3.1	Double-Ring Infiltrometer	16
3.2	Slug-out Test	19
3.3	Discharge	25
3.3.1	Flow Tracker	25
3.3.2	Salt Tracer Test	26
3.3.3	Mini-Flowmeter	28
4	Results and Discussion	30
4.1	Double-Ring Infiltrometer	30
4.2	Slug-out Test	36
4.3	Discharge	41
5	Conclusion and Outlook	49
6	Summary	51
	List of Figures	53
	List of Tables	55

Acknowledgement

First of all the author would like to thank Dr.-Ing. Dirk Radny for giving me the opportunity to work with him, for introducing me to this topic, for his help and discussions at all times. Thanks also to Mrs. Jana von Freyberg for her help with the salt tracer test and the introduction in the study area. Further thanks goes to Prof. Jan Seibert, who agreed to be my supervisor from the University and gave me the chance to write my master thesis extern at the Eawag. I also will thank the whole W+T team from Eawag for their help and support in the field measurements and with computer problems.

A special thanks goes to Mr. Lukas Schmidt for his patience, for his assistance in the field, for the introduction in Latex and the support during the last six month.

1 Introduction

Floods are part of the history of rivers and their landscape. Due to precipitation and snow melt the system is replenished and saturated sometimes. Hence, a faster and larger overland flow occurs and floods emerge. A river highly sensitive to such a scenario is the Thur, due to the fact that it does not have a retentions basin. The Thur reacts fast and dynamically to increased overland flow. Additionally, the Thur river affects the groundwater, due to the water of the river in some parts flows into the groundwater (BAFU, 2013). Hence, it is important to know which components are in the discharge of the Thur river. The Swiss water research institute and internationally networked institution Eawag does research on the Thur river in cooperation with the Eidgenössische Technische Hochschule (ETH) in Zurich in case of the RECORD Catchment project (RECORD = Restored Corridor Dynamics). This project investigates what measures are most effective to influence the river corridor, such that river restoration and groundwater flow systems can help to mitigate the effects of floods and droughts, in particular in the context of climate and global change. The project is centred on the Thur catchment (CCES, 2013). This thesis is integrated in the RECORD Catchment project and located on the Rietholzbach, which is a tributary of the Thur river. The aim of this study is to give an overview of the hydraulic characteristics of a part of the Rietholzbach area. The knowledge about the hydraulic characteristic of a slope of the Rietholzbach helps to understand the hydraulic system in the catchment and the corresponding processes.

The following components form the runoff: precipitation, infiltration, overland flow, baseflow and stream flow. Precipitation is important due to the fact, that it is the added water amount: Thus in case of poor precipitation, no flood occurs. The infiltration defines how much and how fast water infiltrates into the soil and the overland flow is the amount of water that flows directly above the soil into the stream. The water amount flowing from the ground water into the stream is defined as baseflow and the stream transports the water downwards away from an area. The questions addressed in this study are:

- What are the infiltration rates in this pre-alpine area and how do they change in space and time?
- How are the hydraulic conductivities of the subsurface?
- Is there an interaction between ground water and stream flow?

- How do the geology and the different soils influence the hydraulic system in the study area?
- What is the difference of discharge and baseflow in an empty system in comparison to a full system?

The hydrological research catchment Rietholzbach (see chapter 2) has been established and equipped in 1975/76 by the Laboratory of Hydraulics, Hydrology and Glaciology (VAW) of the ETH Zürich, thus a lot of investigations including the Rietholzbach catchment have been performed. “Analysis of the time series of meteorological and hydrological measurements in the Rietholzbach research catchment between 1976 and 2005 with special consideration of the dry summer 2003“ of Grutz et al. (2006) gives an overview of all the studies and summarized data of the Rietholzbach catchment area. The most important earlier results used in this master’s thesis are the geology map of Hottinger & Matter (1970), the soil map of Kuhn (1980) and Germann’s publication “Untersuchungen über den Bodenwasserhaushalt im hydrologischen Einzugsgebiet Rietholzbach“ (1981) and furthermore the summarized studies “Hydraulik der Abflussbildung während Starkniederschlägen“ of Zuidema (1985).

2 Fundamental Principles

2.1 Site Description

2.1.1 Location

As mentioned in chapter 1 the Thur, located in the north-eastern part of Switzerland, is highly sensitive to large precipitation and snow melt, due to the fact that it does not have a retentions basin (Fig. 1). The Thur reacts fast and dynamically to increased overland flow. Additionally, the Thur valley aquifer is one of the largest groundwater systems in Switzerland with a length of 36, a width of 2 km and a depth of up to 20 m and it is mainly fed by the Thur river (Schneider et al., 2011).

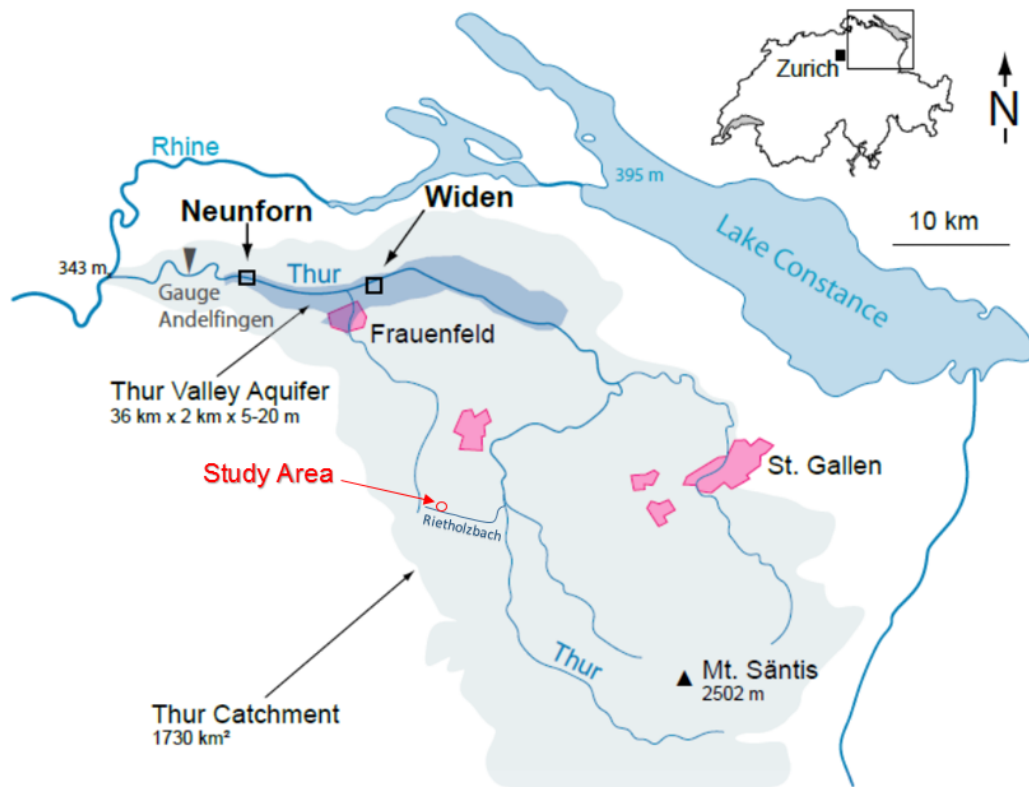


Figure 1: Location of the Thur catchment, the Thur valley aquifer and different test sites at Neunforn (partly restored) and Widen (channelized) as well as the Rietholzbach area in NE Switzerland (Schneider et al., 2011)

As the aquifer is widely used for drinking water abstraction, changes in travel times from river to nearby pumping stations caused by river restora-

tion are a critical issue. The Thur reacts fast and dynamically to increased overland flow and it is characterized by a quickly and highly changing water level. At the measurement station in Andelfingen the mean discharge is $46.9 \text{ m}^3/\text{s}$, whereas the minimum discharge of the Thur is $2.24 \text{ m}^3/\text{s}$ and the maximum discharge is $1130 \text{ m}^3/\text{s}$ (BAFU, 2013). Due to the fact that the Thur affects the groundwater, the knowledge about the entire catchment with a surface area of 1750 km^2 is important, in order to detect the components of the discharge in the river. Hence, this study is located in the catchment of the Rietholzbach creek, which is a tributary to the Thur. The Rietholzbach catchment in the middle of the Thur basin, has an area of 3.31 km^2 and covers an altitude range of 682 to 950 *m*. (Seneviratne et al., 2012)

The area investigated in this study is located in the middle of the Rietholzbach catchment area in the pre-alpine parts of Northeastern Switzerland (Fig. 2 left). More precise it is the area next to the ETH measurement site “Büel“ in Kirchberg. The ETH started a research program at this location in 1975 due to the importance of the Rietholzbach as influent stream to the Thur, which itself is a tributary to the Rhine. Additionally Eawag started two PhD-studies there in 2010. In order to use the measurement methods for obtaining the results in this thesis only a part (70%) of the PhD-Students study area is examined in this study (Fig. 2). The Huwilerbach is a tributary to the Rietholzbach and forms the East boundary of the investigation area (Fig. 2).

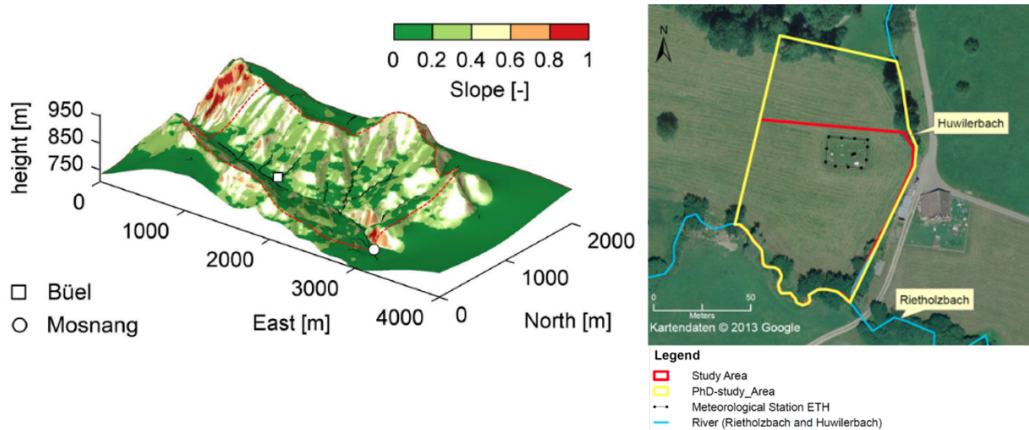


Figure 2: Location of the measurement site Büel in the Rietholzbach catchment (left) and the study area in comparison to the PhD-study area (Seneviratne, 2012)

2.1.2 Geology

The geology of the catchment area from the Rietholzbach is characterized by tertiary deposits of the Upper Freshwater Molasse, which belong to the sedimentation of the almost horizontal stratified Hörnli-Fan deposits “Hörnlichuttfächer“, particularly covering the pre-alpine parts of Northeastern Switzerland (Balderer, 1979).

The study area was created during the Würm-glaciation. Moraines are located next to some quaternary sediments the most important ground-forming components. In figure 3 two kinds of ground can be identified, mainly the common ground moraine and on the right side a wallmoraine reaching into the area of interest. The ground moraine is mostly comprised of silt or fine sand. However the wallmoraine is abundant in gravel and poor in clayey components (Hottinger & Matter, 1970).

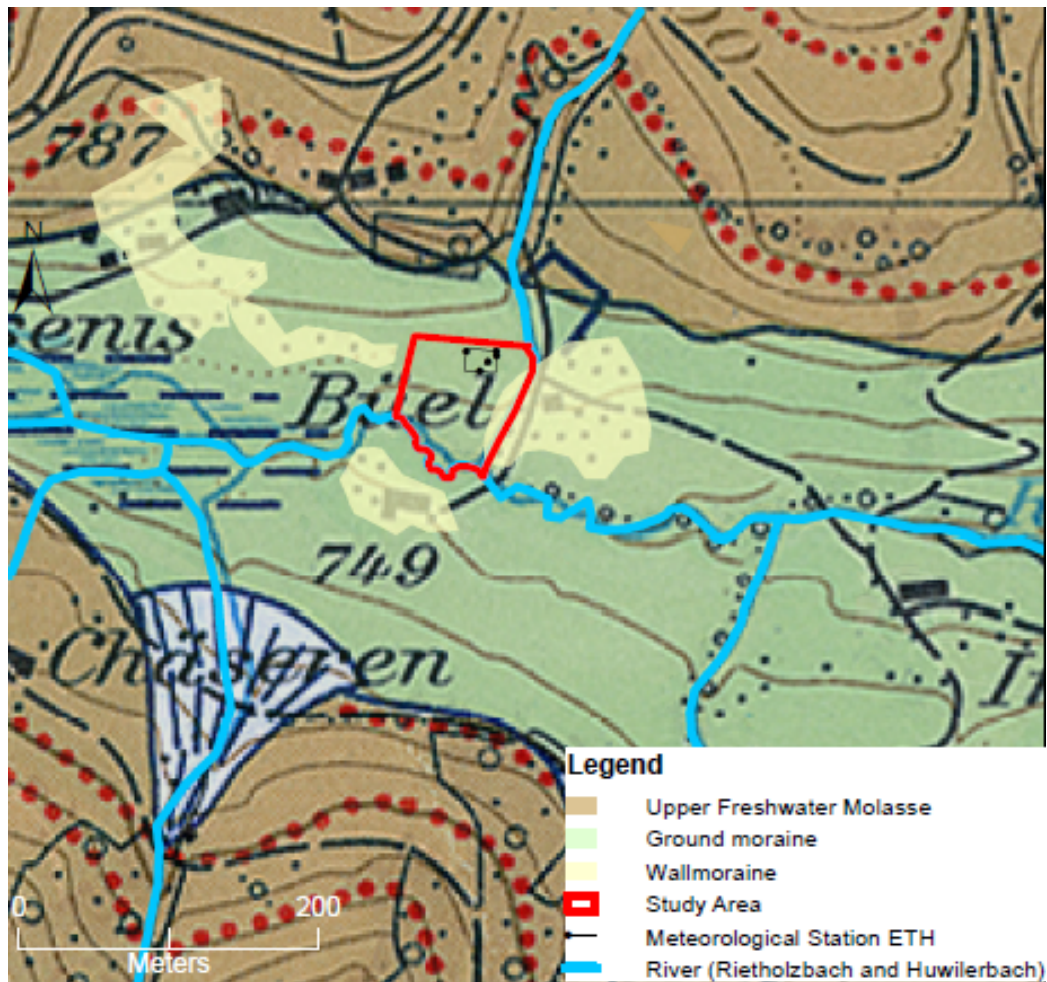


Figure 3: Geology Map of the investigation area (after Hottinger and Matter, 1970)

2.1.3 Soil

Two different main soil types occur in the study area: brown earth and gley. More detailed, six classes of soil appears in figure 4. Orange-coloured is the rather, gleyey brown earth, the so called cambisol in the international soil classification World Reference Base for Soil Resources (WRB). Brown earth is characterized by the process brunification. Next to the river are five different kinds of gley located, in the WRB the so called, gleysol. Gleysols are soils that have undergone prolonged periods of intermittent or continuous saturation with water causing reducing conditions during their genesis. Hence, they occur in depression areas and low landscape positions with shallow groundwater (Scheffer & Schachtschabel, 2010).

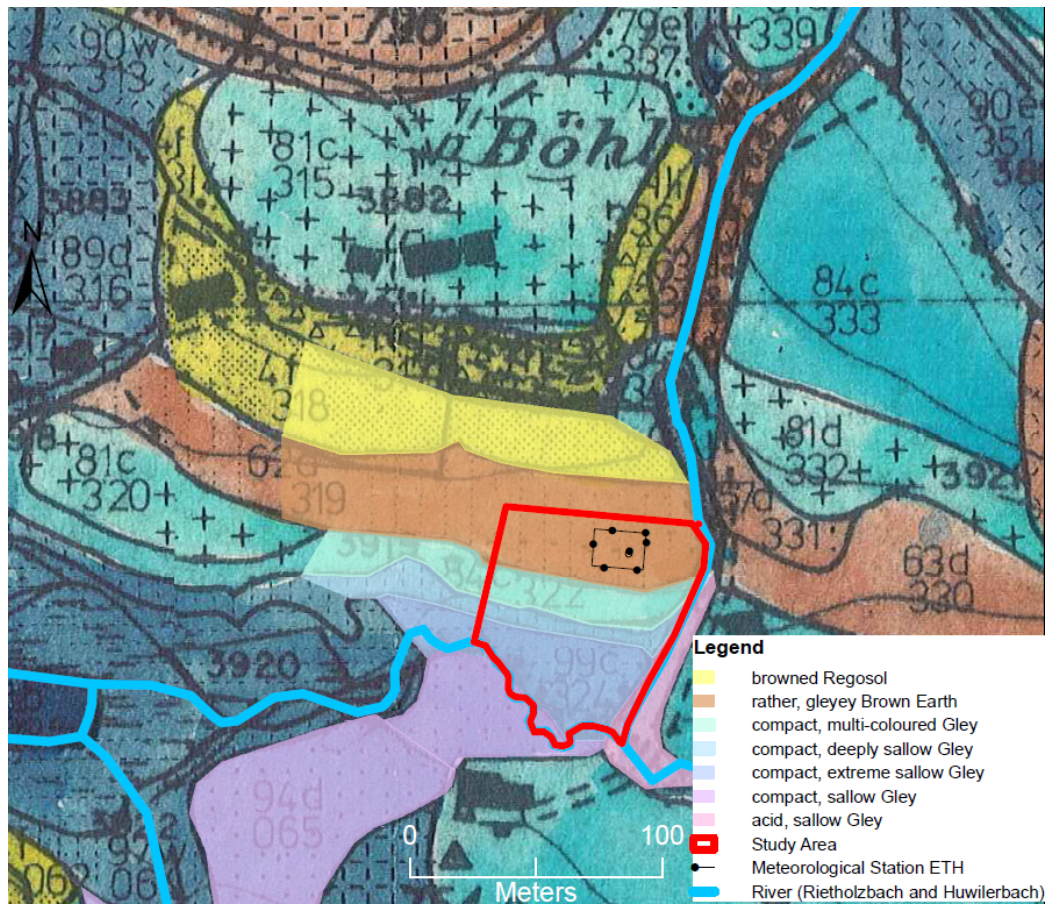


Figure 4: Soil map of the investigation area (after Kuhn, 1980)

2.1.4 Climatology

Grutz et al. (2006) summarized the meteorological and hydrological data from the Rietholzbach (1976-2005) and detected the highest precipitation in the Rietholzbach area in summer (Fig. 5). There are 1459 mm precipitation in total per year. However, the total runoff is smaller during summertime than in winter due to the larger evapotranspiration. The mean temperature monthly value has his peak in July with about 15.7° C and its lowest value with -1.4° C in January.

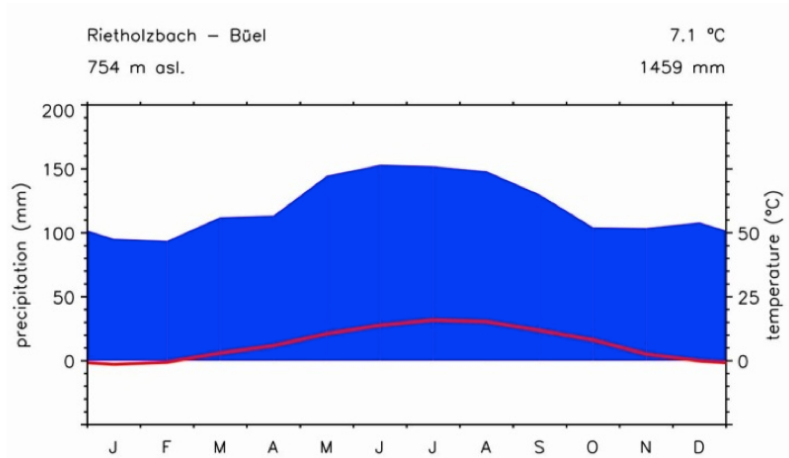


Figure 5: Climate diagram based on data of the time period 1976-2007 (IACETH, 2013)

2.1.5 Land Use

The study area is primarily used as pasture land, thus there is no impervious surface. The grass is cut regularly by a tractor, which leads to compressed soil in the track of the tractor. Only few trees are located along the creek of the study area.

2.2 Theoretical Background

Aim of this thesis is the hydrological characterization of a part of the Rietholzbach area (described in section 2.1). In a hillside as analyzed in this investigation several kind of flows occur. These flows are shown in figure 6. The main flows characterizing a site are overland flow, interflow, baseflow and stream flow. All flows are mainly defined by precipitation and infiltration.

After Zuidema (1985), infiltration is measured in meters of water penetration into the soil per minute and can be described by the following model: Rain that falls on the ground infiltrates the ground-matrix depending on the permeability of the ground. As soon as the precipitation intensity exceeds the infiltration rate in the ground-matrix, there is some residual water decurrent, forming the overland flow.

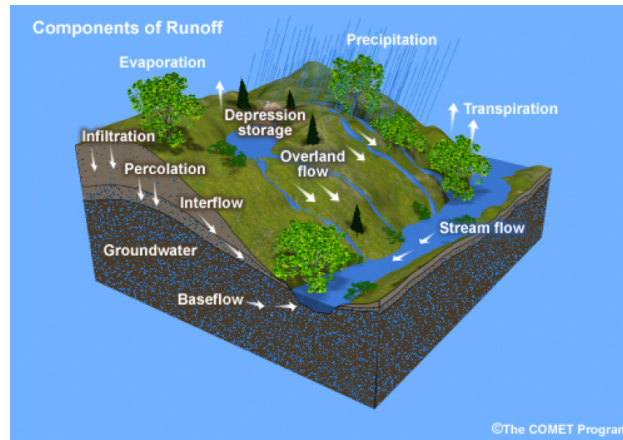


Figure 6: Components of Runoff

2.2.1 Overland Flow

In general, one can distinguish between Horton overland flow and saturated overland flow. Horton overland flow is influenced by the infiltration rate, the better the permeability of the soil, the more water infiltrates into it and the smaller is the overland flow (Ziegler et al., 2001). Hence, the Horton overland flow decreases with growing vertical permeability, whereas a saturated overland flow only appears in case the soil is already saturated and thus no more infiltration occurs. Therefore the saturated overland flow is not affected by the soil permeability. The soil thickness affects the Horton overland flow and the duration until the saturated overland flow is initiated. Obviously, saturating a large soil thickness needs more time than a smaller soil thickness. Velocities of saturated overland flows are high enough to cause the entire overland flow to run into the stream flow, even at slopes longer than 200 m (Zuidema, 1985).

2.2.2 Interflow

The flow parallel to the slope of the soil is called interflow, due to the fact of being located between the overland flow and the baseflow. Interflow exists in the so called subsoil and its velocity depends on the permeability of this subsoil and the inclination of this hillslope. After Zuidema (1985), most of the infiltrated water percolates vertical and forms the groundwater, hence the interflow generally is too small for being considered. Also in this study, the interflow is neglected.

2.2.3 Baseflow

In case the groundwater is hydraulically connected to the stream flow, the water table flows continuously in the stream flow and creates there a potential gradient; the so called baseflow into the stream (Zuidema, 1985). The potential gradient is mostly formed through infiltrated precipitation. Baseflow can be divided into two parts. Firstly precipitation infiltrating into the soil and lifting up the water table and additionally the higher baseflow as a reaction of the higher water table. Both of them are highly sensitive to the distance towards the stream flow.

Propinquity to the Stream Flow

Precipitation infiltrates into the soil, percolates vertical and thus rises the water table. The small distance to the stream flow affects the distinct potential gradient in the stream flow direction. Hence, the baseflow in propinquity to the stream flow is characterized by the infiltration procedure. Regularly, the depth to water table is small, hence it is still more sensitive to the infiltration. (Koskelo et al., 2012)

Remote to the Stream Flow

Depending on the precipitation and infiltration conditions the water table rises. However, the water table reacts delayed in areas far-away from the stream compared to areas next to the stream. This can be explained by the depth to the water table, which is greater in areas remote to the stream flow. Infiltrated precipitation needs more time percolating down to the groundwater due to the larger distance. Additionally, there is always a part of the water kept in the subsoil or flows away as interflow and never reaches the ground water. Hence, the water table raises not only delayed, it rises also less due to the retained water in the unsaturated area. (Eckhardt, 2008)

The baseflow increases by rising groundwater thickness. Due to the lateral transport capability by a stable potential gradient, it grows proportionally to the groundwater thickness. Zuidema (1985) compared the baseflow of two different slope length and detected a decreasing baseflow coefficient with rising slope length. Usually only the water table change next to the stream flow leads to a higher baseflow.

2.2.4 Stream Flow

The before mentioned flows end in the so called stream flow. The stream flow is formed by directly influent water through precipitation and the overland flow as well as by indirectly influent water through interflow and baseflow

(gaining stream). Otherwise, an inflow from the stream into the soil is also possible and the stream flow decreases (losing stream). Depending on these forming factors the stream flow volume changes.

2.2.5 Infiltration

Infiltration is the flow of water into the soil surface and the infiltration rate is defined as the amount of water relative to a given area and a given time enters perpendicularly into the ground (DIN 19682, 2007). John Robert Philip formulated a general flow equation. Based on Darcy's law the model includes the hydrodynamic parameters of soil:

$$i(t) = \frac{\partial I}{\partial t} = k_{sat} \frac{H_0 - H_f(t)}{z_f(t)} = k_{sat} \frac{h_0 - h_f z_f(t)}{z_f(t)} \quad (1)$$

where $i(t)[cm/min]$ is the infiltration rate, $t[min]$ is the time, $I(t)[cm]$ is the cumulate infiltration, $k_{sat}[cm/min]$ is the hydraulic conductivity at the saturation, $H_0[cm]$ is the hydraulic total head at the surface, $H_f(t)[cm]$ is the hydraulic total head at the humidity front level, $z_f[cm]$ is the maximum depth of the humidity front, $h_0[cm]$ is the pressure head at the surface and $h_f[cm]$ is the pressure head of the humidity front. (Philip, 1957)

2.2.6 Hydraulic conductivity

Water moves through soil as saturated and as unsaturated flow. Saturated flow occurs when all pores are completely filled with water respectively the soil is saturated. Unsaturated flow occurs in unsaturated soil, which consists of pores filled with air. Hydraulic conductivity is a soil property that describes the ease with which water can move through pores. It depends on the soil character: porosity and configuration of the soil pores. Saturated flow in this study is defined as K_{sat} and unsaturated flow by K . The quantity of water per unit of time Q , that flows through a column of saturated soil is expressed by Darcy's Law, as the following equation shows:

$$Q = K_{sat} A \frac{\Delta P}{L} \quad (2)$$

where K_{sat} is the saturated hydraulic conductivity, A is the cross-section of the column through which the water flows, ΔP is the hydrostatic pressure difference from the top of the column and L is the length of the column.

The calculation of the hydraulic conductivity in an unsaturated soil is more complex. The gravity has a lower influence, than the differences in the

matrix potential (Philip, 1957). The matrix potential gradient is the difference in the matrix potential of the moist soil areas (lower matrix potential) and nearby drier areas (high matrix potential) into which the water is moving (Brady & Weil, 1999).

3 Methods

In this chapter the methods used for measuring the infiltration rate, the overland flow, the hydraulic conductivity, the baseflow as well as the discharge are described.

3.1 Double-Ring Infiltrometer

The infiltration behaviour of soils, particularly the soil infiltration capacity, is one of the most important processes to understand the hydraulic character of a catchment. The infiltration rate is defined as the amount of water entering perpendicularly into the ground relative to a given area and a given time (DIN 19682, 2007). The infiltration capacity is identified theoretically with the hydraulic conductivity of the saturated soil, so that infiltration measurements can provide estimates of vertical hydraulic conductivity values (Youngs, 1972).



Figure 7: Example of a double-ring infiltrometer construction as used in this study

In order to determine the infiltration rate in the study area described before double-ring infiltration measurements were conducted, since this is a well-established method (Sdiras & Roth, 1987). Double-ring infiltrimeters are commonly used for in situ determination of hydraulic soil properties. It consists of two concentric open cylinders driven 2 – 5 cm in the ground. Testing the infiltration rate works by filling the rings partially with water and periodical measuring the water level while the water in the rings infiltrate into the soil. The double-ring infiltrimeter experiment is carried out until

there is a constant rate of water loss from the inner ring. In order to test on realistic terms, both rings are filled to identical water levels. Hence, no relative water pressure difference between both areas, the inner and the outer ring, is generated and thus equivalent infiltration conditions are given. Thus a realistic precipitation situation for the inner ring is achieved. Due to the fact that in nature the vicinity of the investigated area is also wet and thus additional water infiltration occurs. More important, one minimizes the lateral flow by filling the outer ring with water. For the measurements conducted in this study the infiltration rate was tested by a double-ring infiltrometer with an inner ring radius of 0.15 m and an outer ring radius of 0.25 m .

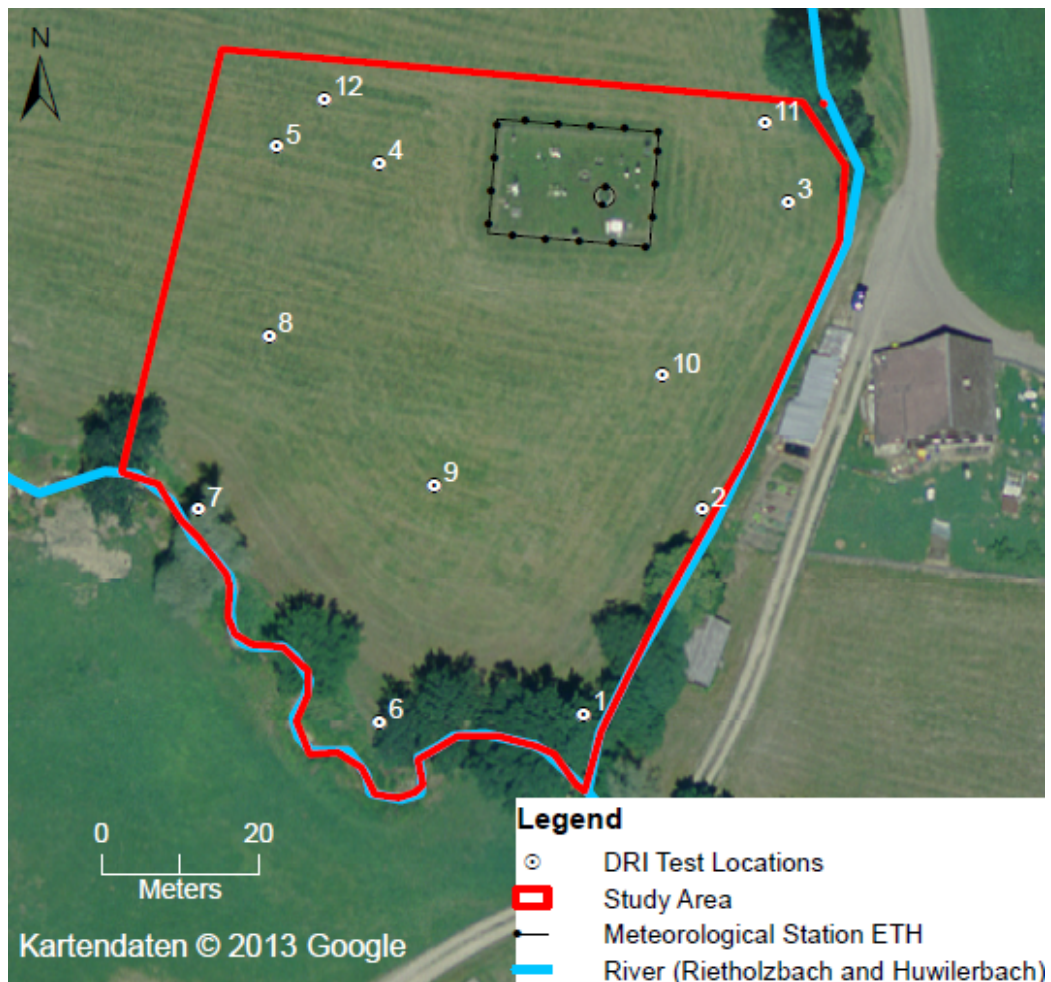


Figure 8: Positions of the conducted double-ring infiltrometer measurements

The measurements were performed on 12 different locations in the study

area (Fig. 8). Initially, a balancing spatial distribution was considered. However, due to the fact that double-ring infiltration measurements are not properly feasible in areas with too large steepness, an equal spatial distribution in the investigation field was not possible. Double-ring infiltration measurements are not practicable in areas with large steepness, due to the resulting unequal water distribution in the rings, which generate uneven hydrostatic heads, manipulating the infiltration rate. Only if the water table is horizontal and parallel to the slope a consistent infiltration is possible. The locations were chosen by its representativity to the vicinity. For this reason one avoided measurements in a tractor line or in a local water-saturated hollow. Both rings of the infiltrometer were driven 2 cm into the soil, around their entire perimeter. This ensures that the rings are densely stacked into the ground and thus no water leaks as overland flow and manipulates the measurements. The rings were both filled with water to an equal height of 15 cm, generating balanced hydrostatic heads and thus creating identical infiltration conditions. In order to minimize the manipulation of the measurements by water flowing from one ring to another between ring and soil, a relative water pressure difference between the two areas was avoided. Thus there is no water loss into the outer ring. Additionally, the purpose of the outer ring is to promote one-dimensional, vertical flow beneath the inner ring (ASTM, 2009). Due to the fact that vegetation influences the infiltration (Zuidema, 1985), it has not been cut for this study. Hence, the measurements were made with vegetation, and the localization was chosen, by representative vegetation for the near surrounding. The water level in the inner ring was measured every three minutes at the same point. Since, the total measurement time at each location was 21 minutes, seven time-dependent water level heights were available. The data analysis was performed using the Green and Ampt model (1911):

$$i(t) = k_{sat} \left(1 + \frac{h_0 - h_f}{z_f(t)} \right) \quad (3)$$

where i [cm/min] is the infiltration rate, k_{sat} [mm/h] is the hydraulic conductivity at saturation, h_0 [mm] is the surface pressure load, h_f [mm] is the pressure load at the humidity front and z_f [mm] is humidity front depths.

In case the water level dropped below a height of 7 cm it was necessary to refill water due to the low water pressure. This was possible since the value of interest in this measurement was the variation of the water level with respect to time and not the total height. The ring depth into the soil was kept constant during the measurement, due to the fact that a change in depth, e.g. hammering on top of the ring, would manipulate the „natural“ infiltration rate.

Green and Ampt (1911) explained in their Paper that the vertical hydraulic conductivity of the saturated soil is nearly equal to the infiltration rate:

$$i(t) = k_{sat} \quad (4)$$

Hence, in this study the infiltration capacity was measured (i.e. the infiltration rate in saturated soil) and these values were set equal with the vertical hydraulic conductivity. The saturated soil infiltration rate values were determined as the constant values of the infiltration rate at the end of a double-ring infiltrometer test.

Interpolation

The results were interpolated and visualized by using the geographic information system software ArcMap (ESRI) with the method “Kriging“. A South African mining engineer Danie G. Krige developed 1951 this interpolation method basing of spatial dependence of the measurement points, so called Kriging. The mathematician Georges Matheron extended this method and formulated the theory of regionalized variables (Dutter, 1985). The Kriging-method assumes that the distance between the reference points or the direction of a reflecting spatial correlation with the aid of variations can be explained on the dently. Firstly, Kriging process the preliminary statistical analysis of the data, second a vario-gram modeling and third the creation of the surface. The Kriging-method is best used by knowing that the data have a spatial correlated distance or directional bias, for this reason this method has been used for the interpolation in this study. Additionally, it is the common used tool in soil science and geology and even in the present investigation.

3.2 Slug-out Test

In order to characterize the baseflow it is of major importance to have detailed knowledge about the aquifer characteristic. A slug test is one of the aquifer test methods commonly used to investigate aquifer parameters (Yeh & Yang, 2006). Slug tests are cheaper than pumping tests and the cost of constructing a slug-body are comparatively low. No laboratory is used to analyze bore cores, since testing the hydraulic conductivity directly in the field is possible. Hence, a simulation of natural and locational processes is not necessary. Slug testing is relatively easy and inexpensive to perform, thus it has been widely done (McElwee, 2002). In this study the wells needed for the testing already existed in the investigation area. Slug tests were conducted along the profile

shown in Fig. 9 in seven different wells along the hill slope.

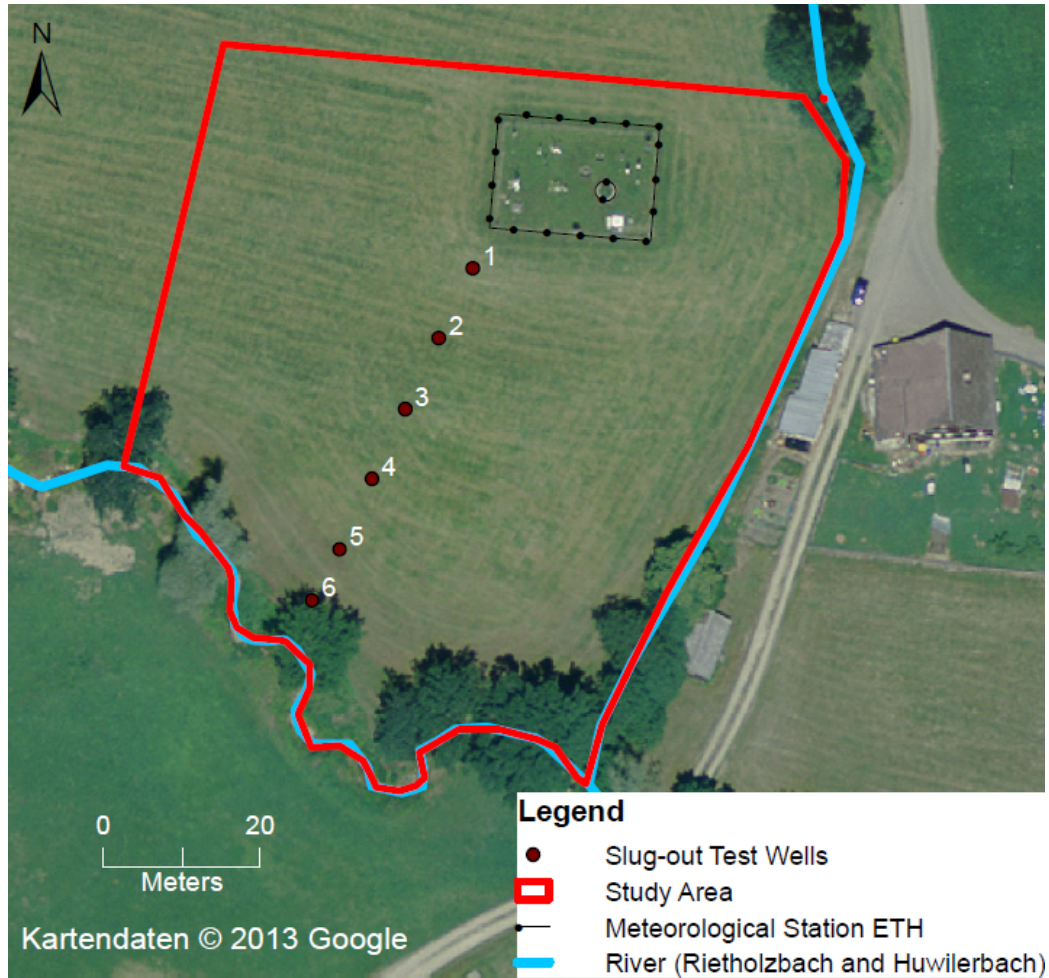


Figure 9: Positions of the slug-out test wells

Monitoring wells are needed for conducting slug tests. A well is like a window on the surface for hydrologists, certain requirements as there are: a well casing, a well screen and a filter pack. All the well cases in this field study have a radius of 0.025 m and consist of two unscreened parts and a screened central section. The screened part is essential for the slug tests. Its openings must not be too small or too big, due to its influence on the conductivity which would thus be predicting an unrealistic conductivity in the test analysis. Hence, the size of the openings are determined by the characteristics of the formation in which the well is screened (Fig. 10). Another important requirement is the filter around the case. In the investigation area, the filters are composed of gravel and not made up of drilled debris, hence it

is called artificial filter pack instead of natural filter pack. The case stabilizes the formation by decreasing the potential for movement of fine material into the well.

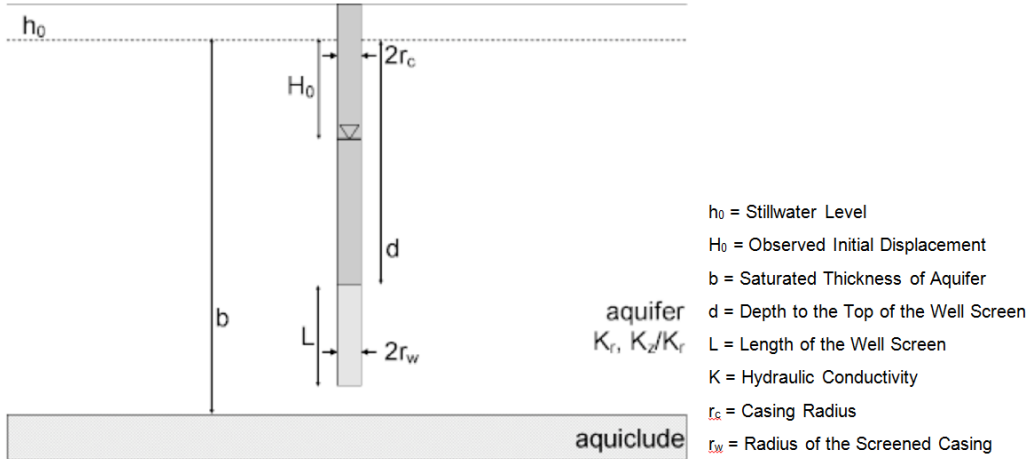


Figure 10: A schematic view of the well constructions (AQTESOLV, 2013)

The principle of slug tests is based on an abrupt artificially created change of a hydrological gradient between a test-well and the ground-water level. The water-level changes due to a falling slug-body pushing the water into the aquifer (slug-in test) or due to a slug-body displacing parts of the water (slug-out test). Characterizing the aquifer is the duration during which the water level returns to the still-water level measured by a logger. The slug-test equipment is easy to handle and only consist of a laptop, one logger, an electric tape and a slug-body. Before starting a slug-test the actual ground-water level in the well was measured using an electric tape. This device consists of a two wires coaxial cable that has electrodes separated only by an air cap at the lower end. The circuit is completed when both electrodes enter the water. A buzzer, light or parameter is used to indicate that the water level has been reached. Depth to the water is read directly from a tape that is fixed to the cable (Butler, 1997). By knowing the water-level, the position of the logger may be calculated in the well and thus it can be fixed at the appropriate location. The logger used for this fieldstudy was a so called pressure-electric conductivity-temperature probe, model DL/N 70 from the manufacturer Sensor Technik Sirnach (STS). After measuring the water depth and fixing the logger in the well the slug-in test was initiated by rapidly introducing the solid object, called slug-body, to the well located nearly 2 cm below the water level. In order to protect the logger from disturbances a distance between the logger and the slug-body is needed. The

slug-body used in this study is a streamlined solid aperture consisting of cast iron with a radius of 0.021 m and a length of 1.03 m . It is fixed onto a rope, its length defines the right position after falling down into the well below the water-level. When the slug-body falls down it pushes the water immediately around the case into the soil. The fact that the radius of the slug-body is nearly as large as the case radius, impeded the water loss above, inside the well. The height of water-level change as well as the duration while the water level returns to the still-water level characterizes the conductivity of the soil. As soon as the water table returns to the same level the slug-out test was initiated. That means, the slug-body is rapidly removed from the well. A watercap accrues and needs to be filled with ground-water. Again the height of water-level change as well as the duration during which the water level returns to the still-water level is used to characterize the conductivity of the aquifer.

The locations of the slug-tests are described above. During the test, some irregular fluctuations, the so called noise could be recognized while performing the slug-in tests. This noise was constantly greater than the noise occurring in the slug-out tests. Additionally, the water table was most often so close to the surface, that a water loss occurred on the top. This is strictly forbidden in a slug test because the duration until the water comes back from the ground is measured and a water loss in the air respectively on top of the soil surface is not measurable. A gravel pack usually forms a zone of higher hydraulic conductivity immediately outside the screened area (Butler, 1997). That is the reason while in areas with low conductivity the slug-out test is more precise than the slug-in test, due to fact that the water is pushed into and above the gravel pack and not only horizontally into the soil. For minimizing the noise and the water loss above only slug-out tests have been conducted in this study. Every well was tested twice.

The performed slug out tests were analyzed with the software AQTESOLV Pro based on the method invented by Bouwer & Rice (1994). Geometry and symbols of wells in this field study are shown in figure 10. Bouwer & Rice (1994) developed a method determining the hydraulic conductivity K of unconfined and confined formations. This method is based on the mathematical model defined as follows.

The flow into the well at a particular value of $\Delta h = h(0) - h(t)$ can be calculated by modifying the Thiem equation to

$$Q = 2\pi K L \frac{h(0) - h(t)}{\ln \frac{R_e}{r_w}} \quad (5)$$

where $Q[m^3/s]$ is the flow into the well at a certain value for $h(t)[m]$ &

$K[m/s]$ is the hydraulic conductivity of the aquifer, $L[m]$ is the height of the portion of well through which water enters, $R_e[m]$ is the effective radius over which $\Delta h[m]$ is dissipated and $r_w[m]$ is the horizontal distance from well center to original aquifer (radius of casing plus thickness of gravel pack). Equation 5 is based on the assumptions that lowering of the water table in the area of the well is small enough to be neglected, the flow above the still water level in the capillary can be ignored, the well losses are also negligible and thus the aquifer is assumed to be homogeneous and isotropic. In this investigation area all these requirements are assumed according to earlier studies from Germann (1981), Grutz et al. (2006) and Weiler & Naef (2003). For the rebound of the water table to the still water table after a slug-out test, the following equation can be applied

$$\frac{dh}{dt} = \frac{-Q}{\pi r_c^2} \quad (6)$$

where $r_c[m]$ defines the radius of the region of the well in which the water level rises. Bouwer & Rice (1994) indicate that in case the hydraulic conductivity of the gravel pack zone is significantly higher than that of the aquifer, the porosity in the permeable zone must be included in the cross-sectional area of the well, meaning r_c has to be replaced by an equivalent value

$$r_{eq} = [r_c^2 + p(r_w - r_c)^2]^{1/2} \quad (7)$$

where p is defined as the porosity of the gravel pack. Combining equation (Eq. 5) and (Eq. 6) and integrating the obtained equation, then additionally applying this integrated equation between limits $h(0)$ at $t = 0$ and $h(t)$ at $t[s]$. Solving for K yields

$$K = \frac{r_c^2 \times \ln \frac{R_e}{r_w}}{2L} \times \frac{1}{t} \times \ln \frac{h(0)}{h(t)} \quad (8)$$

where $h(0)$ is the maximum water table change in the well at the slug-out test begin $t_0 = 0$ and $h(t)$ the height difference in terms of the still water table at time t . Due to in this study all wells have a gravel pack with a higher conductivity than the aquifer, r_c has to be replaced by r_{eq} (Eq. 8):

$$K = \frac{r_{eq}^2 \times \ln \frac{R_e}{r_w}}{2L} \times \frac{1}{t} \times \ln \frac{h(0)}{h(t)} \quad (9)$$

All the parameters are simple to define by measurements directly in the field and the information available about the well construction. The only parameter that has to be assumed is R_e . R_e is the effective radial distance

over which head is dissipated, it is also the distance away from the well over which the average value of K is being measured (Fetter, 1994). This not measurable parameter is automatically calculated in the AQTESOLV software.

The AQTESOLV software program is one of the leading software for the design and analysis of aquifer tests. The software version AQTESOLV Pro consists of the most comprehensive set of aquifer test analysis tools including advanced solutions and features not found in other commercially available software packages (AQTESOLV, 2013). With the Slug Test Wizard the well parameters and the measured data by logger are inserted step by step. In the end the model estimates the parameter K [m/sec] and visualizes this in a diagram (example shown in figure 11).

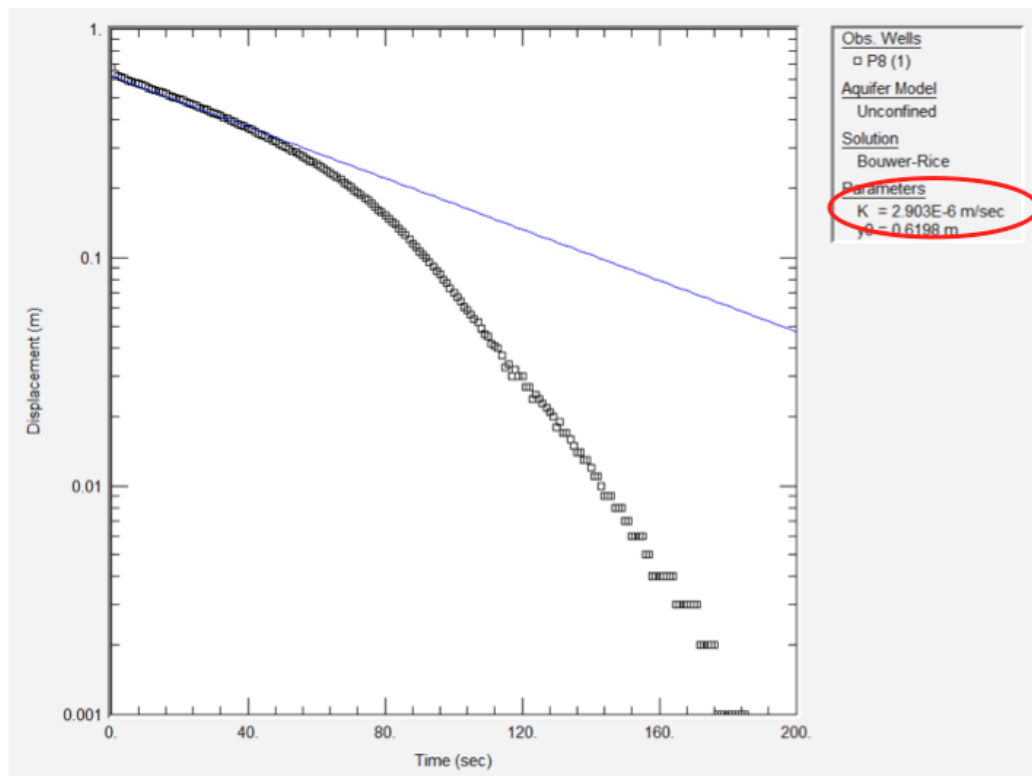


Figure 11: Example of an AQTESOLV Diagram

As the results of the double-ring infiltrometer measurements, the results of the slug-out tests were interpolated and visualized by the software ArcMap with the Kriging method (see also section 3.1).

3.3 Discharge

The aim of the stream flow investigation was to detect the discharge on different locations along the stream. Hence, by detecting variations in the discharge, interactions between the slope and the stream flow can be discovered. Hence, it can be answered if the Rietholzbach is a gaining or a losing stream in the investigated stream section.

3.3.1 Flow Tracker

In this study the stream flow was tested by different measurement methods. The first measurements were taken using the so called Flow Tracker (Son Tek). This is a device consisting of a sensor, measuring the velocity of the stream flow using the Doppler effect based on swimming particles in the water (Fig. 12). To calculate the discharge, the water depth and width have to be available and inserted into the device. The apparatus considers error inaccuracy by itself and is easy and comfortable to use in the field.



Figure 12: Schematic figure of a Flow Tracker (Quantum Hydrometrie, 2012)

The Flow Tracker is highly sensitive to the adjustment of the height of the sensors. Due to the uneven brook bed filled with gravel the correct adjusting appears to be difficult. The more uneven and wider the brook bed,

the less precise are the measurements. Additionally, the measurement accuracy depends on the amount of particles in the water. The water of the Rietholzbach sometimes contains not enough particles and this may lead to imprecise measurements. Since greatly varying values resulted from measurements performed in a short time span on the same location by using the Flow Tracker, the discharge of the stream flow was quantified by a salt tracer test.

3.3.2 Salt Tracer Test

In this study sodium chloride (NaCl) has been used as salt tracer. It splits up into the cation Na^+ and anion Cl^- when dissolved in water and can thus be used to manipulate the electrical conductivity of the water. The common availability of salt, relatively low costs, simple handling and the potential for continuous measurements are the advantages of a salt tracer (Leibundgut & Seibert, 2011). Since, the electric conductivity is linearly dependent on the salt concentration, it is easy to measure.

At an input location, a precisely defined amount of a salt is fed into the water. The electric conductivity, which is a measure of the diluted concentration, is measured by a logger on a cross section downstream of the flow. The distance between input and measuring point should ensure the complete mixing of the salt tracer with the stream water. The observed concentration of the measuring point determines the dilution. Since the input amount of salt is known, it is possible to calculate the stream flow using the dilution value.

Five different locations along the stream flow have been tested in the study area. Those locations were positioned at the border of soil change in order to detect variations induced by the inflow behaviour of different soils onto the stream flow (Fig. 13). For the following thesis the relevant three soils for the discharge measurements were called, yellow-soil, instead of “compact, sallow gley“, green-soil, instead of “compact, extreme sallow gley“ and orange-soil, instead of “acid, sallow gley“. Two loggers were installed at every measurement location. The measurements have been conducted with a constant input of the NaCl solution of 0.22 l/s .

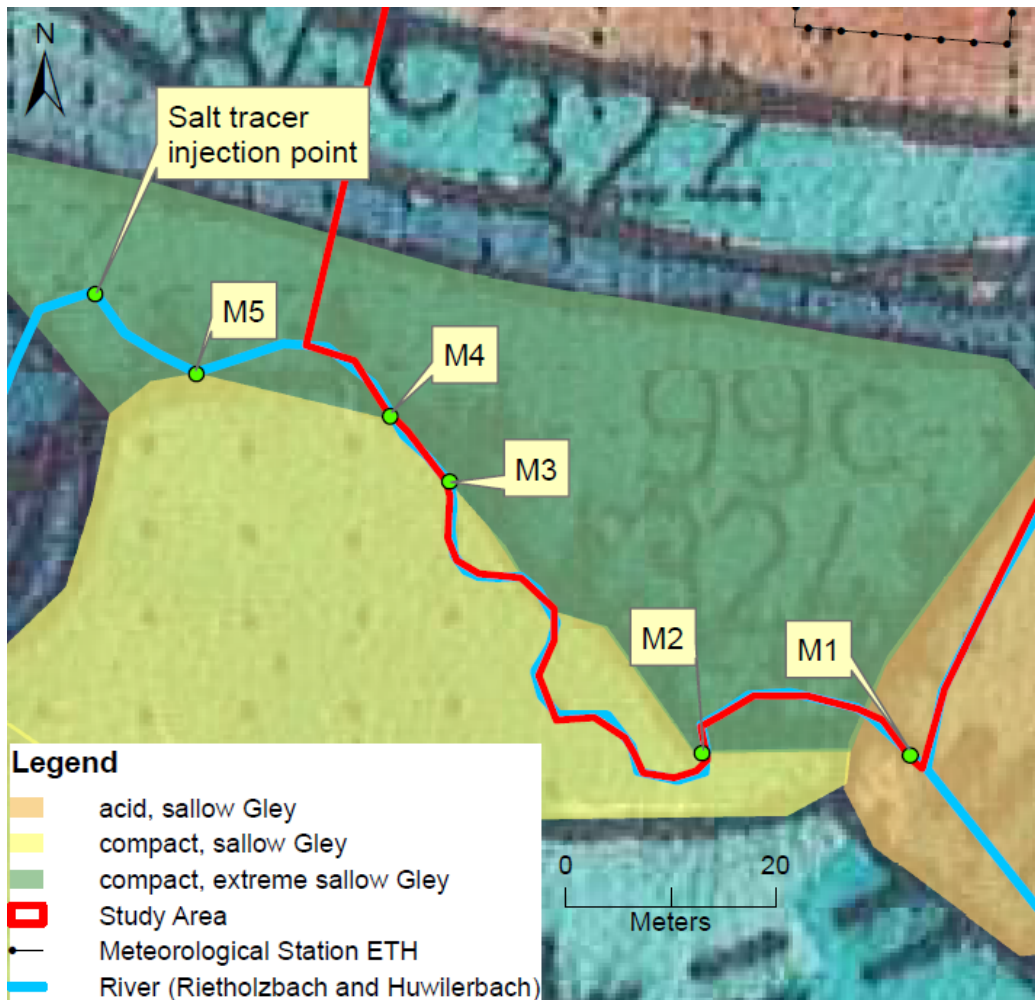


Figure 13: Measurement points (M) of the discharge measurements (Kuhn, 1980)

Before entering the salt tracer, the loggers were calibrated with water from the Huwilerbach. This was possible, since the conductivity of the Huwilerbach differs not much from the conductivity of the Rietholzbach. After locating two loggers (measuring interval: 10 sec) on every measurement point, a continuous measurement of the electric conductivity was initiated, lasting for a period of 30 minutes. In order to keep the input amount of the salt tracer exactly constant, a metering pump was used ($q = 0.22 \text{ l/s}$). The constant tracer input must continue until the tracer concentration reaches a plateau at all measurement points. Additionally to the installed loggers the conductivity was measured with handloggers, in order to observe the behaviour of the salt tracer in the stream flow. Thus in-time measurement of the conductivity was performed, which gave the opportunity to determ-

ine the experimental duration precisely. As soon as the conductivity values decreased and reached background values of the Rietholzbach water the test was finished. The discharge than can be calculated from the difference in salt concentration at the plateau values and the original concentration of the Rietholzbach-water.

For the calibration of the loggers a volume of 10 ml, of a solution of 10 g NaCl dissolved in 1 liter water, was added into a bucket filled with 3 liter of Huwilerbach water and all the loggers. After one minute, another 10 ml of the salt water solution was added. One minute after that another 20 ml of this solution and at last again 20 ml of this solution were added into the bucket one minute later.

By adding a trendline on the measured points in the bucket one obtains a linear equation, which is used to calculate the salt concentration in the Rietholzbach based on the electric conductivity [mS/cm] measured by the installed loggers in the Rietholzbach.

The stream flow amount there can be calculated by the following equation

$$Q = qC_1C_2 \quad (10)$$

where $Q[l/s]$ is the discharge, $q[l/s]$ is the inflow rate of the input solution, $C_1[mg/l]$ is the concentration of the input solution and $C_2[mg/l]$ is the concentration increase, corresponding to the measured plateau concentration minus the natural concentration of the Rietholzbach. (Jardani et al., 2013)

3.3.3 Mini-Flowmeter

The stream velocity was also measured using a MiniAir2 Schiltknecht (Fig. 14). The stream velocity can be obtained by means of conversion tables that relate the rotational speed of the blades and the stream velocity to each other. To calculate the discharge, the velocity has been multiplied with the water height and the width of the measured part. This is measured and calculated for every 10 cm of a cross-section. The measurements with the Mini-propeller were conducted in an empty system only on location 1 and in a full system at every 5 measurement locations (Fig. 13).



Figure 14: Mini-Flowmeter (MiniAir2 Schiltknecht)

4 Results and Discussion

In this chapter all important results obtained by different tests about the infiltration, hydraulic conductivity and stream flow are described. Firstly, the analysis performed with the double-ring infiltrometer is discussed.

4.1 Double-Ring Infiltrometer

In this chapter, only some characteristic infiltrometer measurements are presented and discussed. All conducted infiltrometer measurements and their results are shown in figure 18.

The first described example is a typical example for the first five double-ring infiltration (ID: DRI 1 - DRI 5) measurements. It is the second measurement (ID: DRI 2) and has been conducted on the right hand side in the middle of the slope next to the Huwilerbach (Fig. 19). The soil is a compact sallow gley. Figure 15 shows the infiltration rates of the second double-ring infiltrometer test. The scatter-plot illustrates a high infiltration rate initially and gradually a lower infiltration rate, i.e. the water infiltrates fast in the beginning and then the infiltration rate slows down. Usually the infiltration rate slows down until it stays constant. Hence, the constant values in the end exhibit the infiltration rate of saturated soil and can be equalized to the hydraulic conductivity in the vertical direction, as explained in chapter 3.1. However, in case of the second double ring infiltrometer measurement (ID: DRI 2) it can be seen clearly, that the end-infiltration rate is not constant. Hence, it was assumed that the duration of the test was long enough to saturate the soil and the last value then represents the saturated infiltration rate. Looking at figure 15 in its entirety, the values do not vary greatly. This is an evidence for a nearly saturated soil.

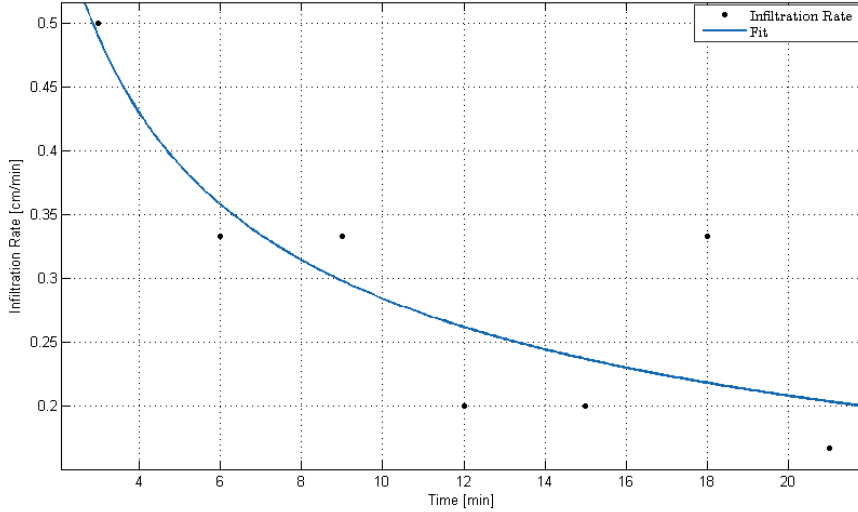


Figure 15: Double-Ring Infiltrometer Measurement 2

The first five measurements have been conducted on the 24th June 2013 in rainy conditions. During the days before the measurements were taken, the weather was sunny and without precipitation, hence the soil moistening was initiated in the afternoon of the 24th June 2013, when rain started to occur. More double-ring infiltrometer tests were conducted two days later at the 26th June 2013, by higher soil moisture conditions, however without precipitation. A typical example for the second measurement day is the measurement number 10, which shows constant values (Fig. 16). Though the values at $t=15$ minutes and 18 minutes do not fit well, all the other numbers show a constant infiltration rate of 0.333 cm/min . After 12 minutes of measuring the infiltration rate drops to 0.0167 cm/min and three minutes later it jumps up to 0.05 cm/min . Following this, again a constant infiltration rate is observed (Fig. 16). As exposed in the original data the difference of the water head was smaller than a millimeter within three minutes. Measuring the exact values with an resolution of mm was not properly possible. Hence, due to this very low and not properly measured variation these values have been ignored. Since, the values are constant starting from the beginning the soil seemed already saturated.

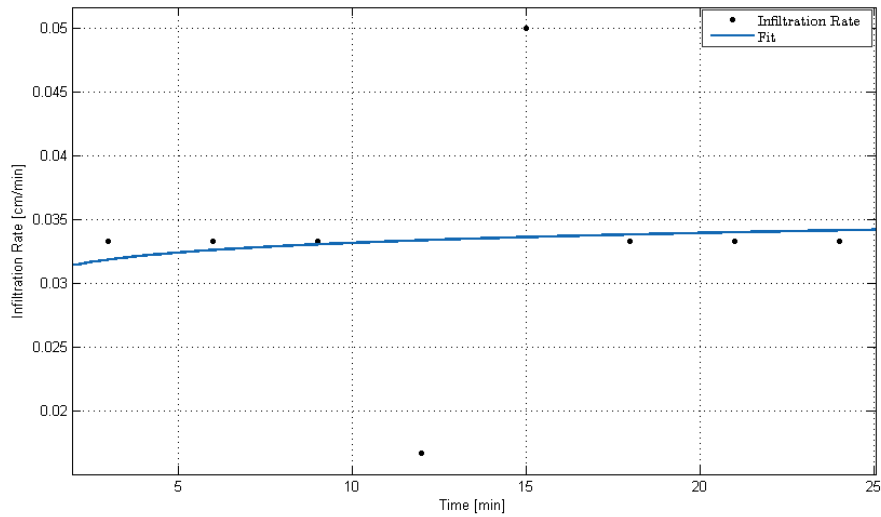


Figure 16: Double-Ring Infiltrometer Measurement 10

The most untypical trendline is shown in figure 17 (test no. 9). This test was conducted on a plane region in the middle of the investigation area. While all the other double-ring infiltrometer tests demonstrate a concave graph, this graph is illustrated convex. Observing the values in figure 17 nothing is greatly conspicuous, the values vary between 0.05 and 0.1 cm/min . Nevertheless by observing the scatterplot it is remarkable that the infiltrations rate values increase with the duration of the test. This effect can most likely be explained by two leaking rings. While both rings are leaking, water comes out faster and faster, which thus predicts an increasing infiltration rate.

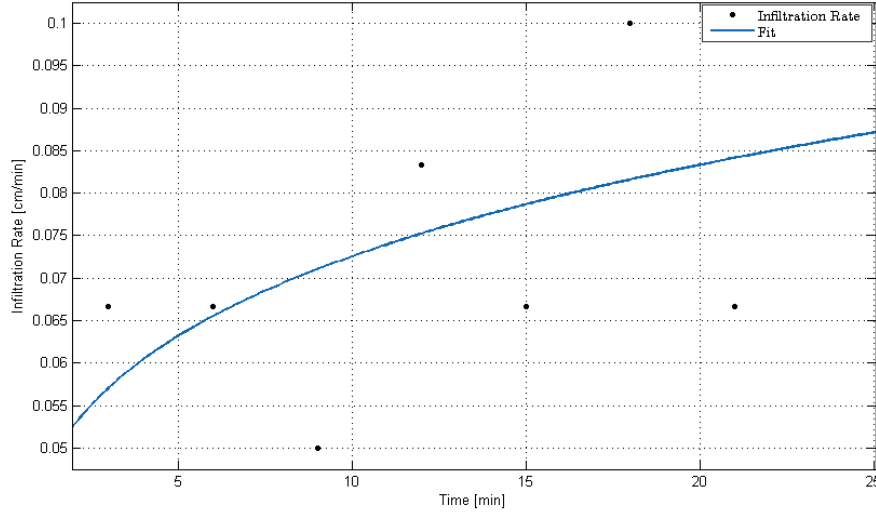


Figure 17: Double-Ring Infiltrometer Measurement 9

Figure 18 shows all double-ring infiltration measurements and their corresponding trendlines. The highest measured infiltration rate in the investigation area is 1.5 cm/min . Due to the fact that only the infiltration rate in saturated soils are interesting for this study, just the end-values are considered (chapter 3.1). Thus the highest value found is 1 cm/min of double-ring infiltrometer measurement number 12. The lowest infiltration rate detected was 0 cm/min at location number 6, however the lowest properly measurable value in the field was measured on the tenth measurement with a value of 0.0333 cm/min . Comparing the trendlines of the measurements 1-5 with the trendlines of the measurements 6-12 it can be observed that the graphs are steeper in the measurements 1-5 compared to the graphs of the measurements 6-12. Hence, the soil was more saturated on the second measurement day than during the first measurement day. The ETH soil moisture measurements during the last week of June confirm this assumption. The graph in figure 18 shows that measurement number 4, 5 and 12 have significantly higher values of infiltration rate compared to the other measurements. Thus it can be concluded, that different infiltration conditions exist in this region compared to the residual area. In comparison to the soil-map of Kuhn (1980) the soil in this region is defined as a rather, gleyey brown earth and the residual investigation area consists of different gley soils. Brown earth has usually a higher hydraulic conductivity in comparison with gley-soils (Scheffer & Schachtschabel, 2010), hence a higher infiltration rate can be observed. An additional reason for this particularly high infiltration values are

macro-pores. They were detected in this area by Germann (1981) and Grutz (2003). Macro-pores influence mainly the infiltration process in the beginning of the measurement. In saturated conditions they lose their influence on the vertical infiltration. The deepest values were measured in the lower part of the slope. The soil in this region is highly gleyey and is characterized by a comparatively low hydraulic conductivity.

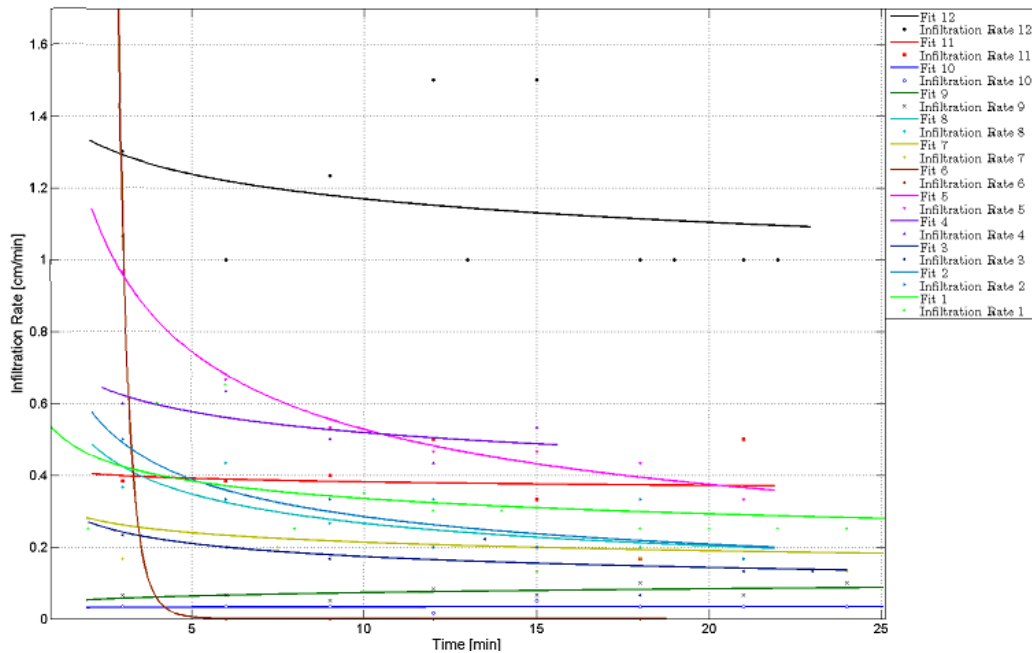


Figure 18: Infiltration rate over time of all conducted double-ring infiltrometer measurements

The interpolated data are visualized in figure 19. The data correlates very well to the soil map (Kuhn 1980). The dark green area is defined by the lowest infiltration rates and the white area is characterized by the highest infiltration rates. It is also possible to recognize that the infiltration rate does not only change by the slope height. Also the soil type has an impact on the infiltration rate. This is discernible in the lower part of the study slope. On the right part of the area, the infiltration rates do not change parallel to the contour lines. This issue can be explained by the geology of the study area (Fig. 3). A wallmorain reaches into the right side of the investigation area, which implements a different soil, as the residual area, which is formed by a ground moraine. Due to the fact that the wallmorain is formed with less clayey elements compared to the ground moraine, the soil is less gleyey and thus shows a higher hydrological conductivity respectively a higher infiltration rate.

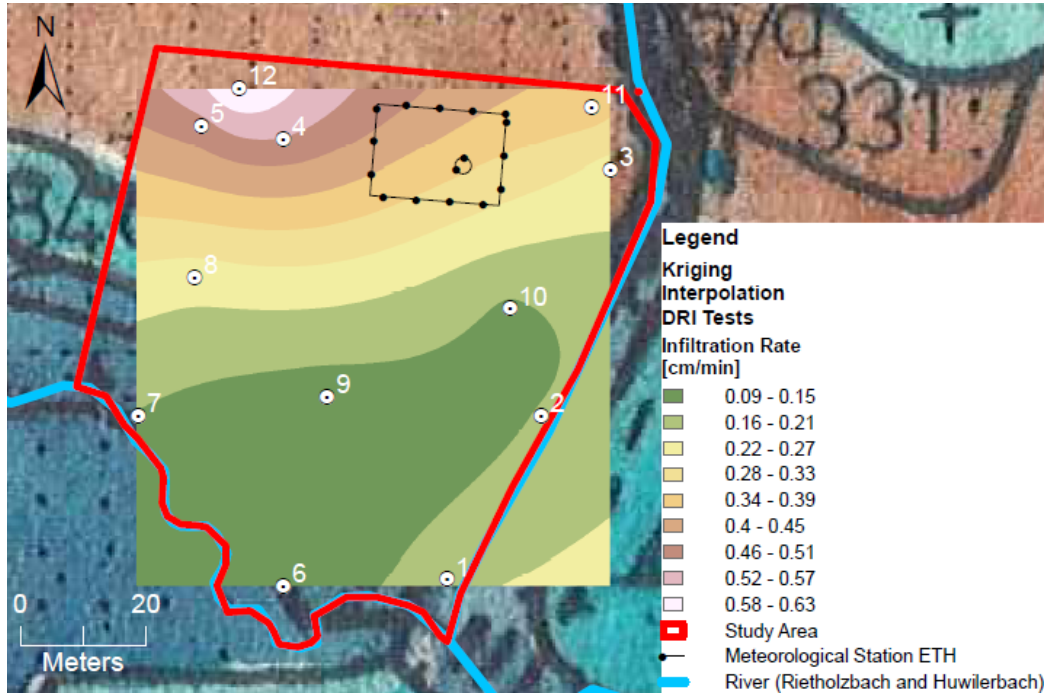


Figure 19: Interpolation Map of the Double-Ring Infiltrometer Measurements, Base map (Kuhn, 1980)

Infiltration and Overland Flow

Based on the interpolation map the study slope is split into nine sections with similar infiltration rates in one section. Due to the decreasing infiltration rate top down, an increasing overland flow is expected in the lower parts of the hill slope. For calculating the potential, total infiltration rate over the investigated slope, each of the nine areas was multiplied by the responsible average infiltration rate of each section:

$$A \times i_{avg.} = W \quad (11)$$

The sum of these resulting nine different infiltration rates gives the total potential amount of water that can infiltrate W_{total} (Tab. 1).

Table 1: Potential infiltration rate in the study area

<i>Area</i> (Colour in Fig. 19)	$A[m^2]$	$i_{avg.}[cm/min]$	$W[m^3/min]$
Green	1984.2	0.12	2.381
Light Green	1562.8	0.185	2.891
Yellow	702.85	0.245	1.722
Dark Yellow	491.9	0.305	1.500
Orange	493.5	0.365	1.801
Dark Orange	354.2	0.425	1.505
Brown	248.1	0.485	1.203
Pink	127.5	0.545	0.695
White	38.6	0.605	0.234
Total	6003.65	0.36	13.933

As mentioned in the fundamental principles the overland flow occurs as soon as the precipitation rate is higher than the infiltration rate. Due to the fact that during saturated conditions $13.933 m^3/min$ water can infiltrate over the entire slope with an area of $6003.65m^2$, the following equation can be used:

$$\frac{W_{total}}{A_{total}} = i_{total} \quad (12)$$

In the case of this study, the overland flow occurs in saturated conditions, when the precipitation rate increases above $0.23 cm/min$. The amount of water that flows, in form of overland flow over the soil directly into the stream, can be calculated by the precipitation rate in the entire slope minus the total amount of water that infiltrates:

$$mP \times A_{total} - i_{total} \times A_{total} = cO \quad (13)$$

where cO is the calculated overland flow and mP is the precipitation rate.

4.2 Slug-out Test

The slug-out tests were conducted and analyzed according to the description in chapter 3.2, the results of these tests are described and discussed in this chapter. The measurements were achieved in the middle of the investigation area along a profile (Fig. 9). Those wells were already drilled for a Doctoral-Thesis, due to this fact, the names respectively the numbers were given before

and do not have a specific meaning. The following parameters were measured and used to analyze the slug-out tests. The observed initial displacement respectively the change in water level from static H_0 , the static water column height H and the saturated thickness of the aquifer b , measured from the aquifer base to the static water level. Additionally, the depth to the top of the well screen d and the length of the well screen L which includes perforated intervals. The investigated aquifer is an unconfined aquifer. The parameters of the wells 1-5 could be easily defined and analyzed for calculating the hydraulic conductivity (Tab. 2).

Table 2: Well 1-5

Well	Hydraulic Conductivity [m/s]
1	1.02×10^{-4}
2	3.30×10^{-5}
3	7.63×10^{-6}
4	4.45×10^{-6}
5	3.13×10^{-6}

However, the calculation of the hydraulic conductivity of well number 6 and number 8 was not as straight as for well 1 to 5. Both wells are located next to the river in a saturated gley soil, the before defined aquifer depth from a PhD work was too low to analyze the measured data. Due to the fact that at this location, b (the saturated thickness of aquifer measured from the aquifer base to the static water level) had a negative value (Fig. 20), analyzing the data with the Bouwer and Rice method of 1976 was not possible.

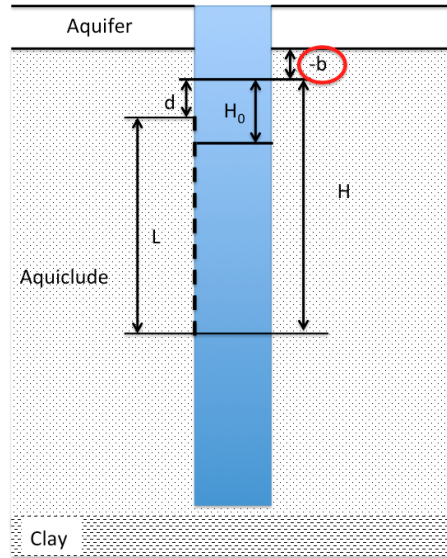


Figure 20: Schematic view of well number 6 with the negative b value

Even other methods as Cooper-Bredehoeft, the Ferris-Knowles method or the Hvorslev method are not able to analyze data with a negative b. For this reason the aquifer was redefined. The saturated and highly gleyey soil, before defined as the aquiclude, was redefined as the new aquifer and the lower located clay soil, was defined as the aquiclude. Due to the fact that Bower (1989) found out that the equation of Bouwer and Rice (1976) also can be used for hydraulic conductivity analysis of aquifers with a particularly low conductivity, the data were analyzed, as well as the wells of number 1-5, with the equation of Bower and Rice (1976) and the redefined parameters.

Table 3: Well 6-8

Well	Hydraulic Conductivity [m/s]
6	2.30×10^{-6}
8	8.73×10^{-6}

The resulting hydraulic conductivity of well 8 seems not trustful. A comparatively high hydraulic conductivity occurs in a gley soil, which is normally characterized by a low hydraulic conductivity. Additionally, well number 6, which is next to well 8, has a comparatively low hydraulic conductivity. A locational specific different hydraulic conductivity is not expected. Thus a distortion of the measurement trough the gravel pack is assumed. Hence, the hydraulic conductivity value of well 8 is ignored in the following.

By comparing the results of the K -values with the distance to the stream (Fig. 21), an exponentially increasing hydraulic conductivity is recognizable: The nearer to the stream, the lower is the hydraulic conductivity.

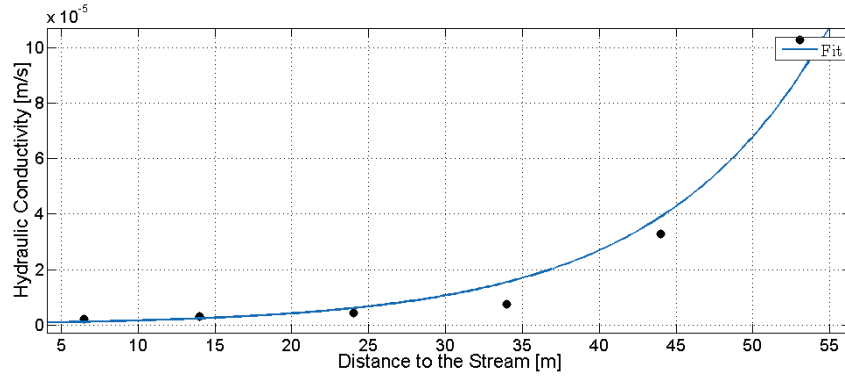


Figure 21: Hydraulic conductivity vs. the distance to the stream

In other words there is an exponential correlation between the distance to the stream and the hydraulic conductivity. This correlation can be fitted with an accuracy of $R^2 = 0.92714$. The larger the distance to the stream, the higher is the hydraulic conductivity. This circumstance can be explained by the in chapter “Fundamental Principles“ described fact, that the hydraulic conductivity depends on the soil character: porosity and configuration of the soil pores. The soil map of Kuhn (1980) clearly shows that the soil changes by the distance to the stream. It becomes dryer and less gleyey, hence the soils hydraulic conductivity increases with the distance. Thus, the correlation between distance to the stream and the hydraulic conductivity values is given.

As already the double-ring infiltrometer measurements, so were the results of the slug-out tests interpolated by the software ArcMap (ESRI) with the “Kriging“method. Figure 22 shows a significant change of soil upwards the slope. A realistic geostatistical interpolation is hardly possible, due to the fact that the measurements were conducted in one line along the profile. Hence, the left and right part of the interpolation map have a larger inaccuracy than the parts next to the measurements. It is assumed, that the borders of the responsible areas are more horizontal and parallel to the stream flow than it is shown in the interpolation map.

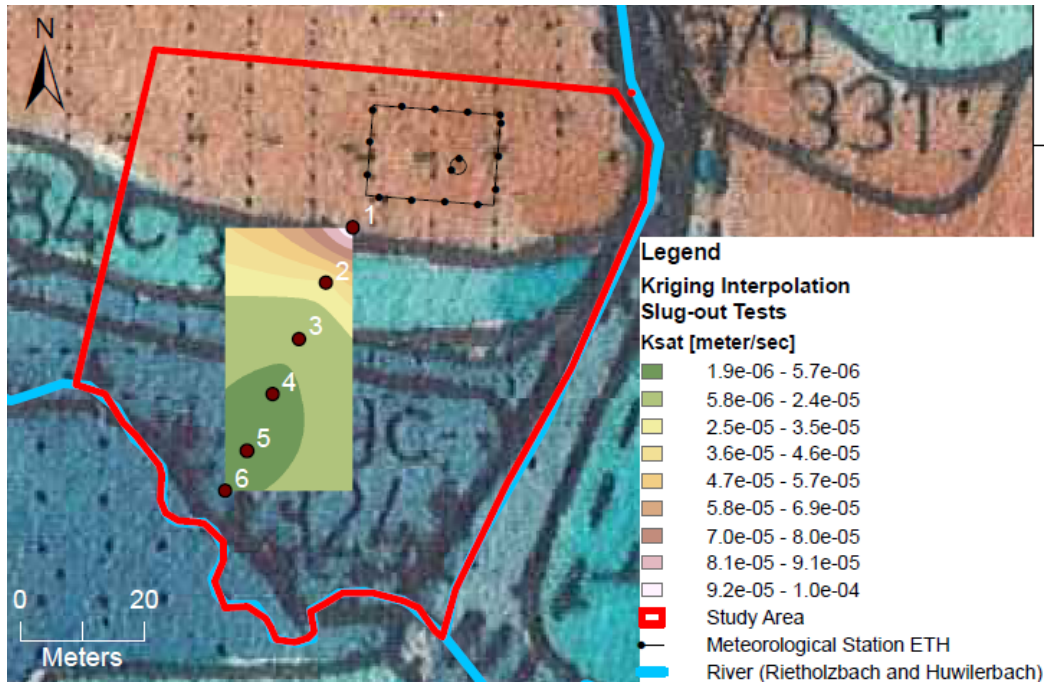


Figure 22: Interpolation Map of the Slug-out Tests
Base map (Kuhn, 1980)

The German Institute for Standardization (DIN) characterizes the K -values by a pass band (DIN 18130, 1998). As example DIN defines the range of K -values of $10^{-2} - 10^{-4} m/s$ as highly permeable. The range of $10^{-4} - 10^{-5} m/s$ is defined as a permeable soil and a range of $10^{-6} - 10^{-8} m/s$ as slightly permeable. Table 4 shows the DIN pass band classification on the basis of the hydraulic conductivity compared to the soil classification of Kuhn (1980) based on field measurements. The classified soils of Kuhn (1980) are characterized by the permeability characteristics which is confirmed by the pass band classification of DIN based on the hydraulic conductivity values.

One aim of this study was to detect an interaction between stream flow and ground water. This is relevant for the discharge. If some water flows in form of ground water, into the stream, the so called baseflow, the discharge increases. However if some water flows from the stream into the ground water, the discharge decreases. It is not possible to detect the baseflow by the slug-out measurements. However, these give an overview about the hydraulic conductivity in the subsurface, which influences the baseflow. For detecting an interaction between the ground water and the stream different discharge measurements were conducted.

Table 4: DIN-Classification (DIN 18130, 1998) vs. Kuhn-Classification (Kuhn,1980)

GWM	Hydraulic Conductivity [m/s]	DIN Pass Band Classification	Kuhn's Soil-Classification
1	1.02×10^{-4}	highly permeable	Brown Earth
2	3.30×10^{-5}	permeable	Multi-coloured Gley
3	7.63×10^{-6}	slightly permeable	Sallow Gley
4	4.45×10^{-6}	slightly permeable	Sallow Gley
5	3.13×10^{-6}	slightly permeable	Sallow Gley
6	2.30×10^{-6}	slightly permeable	Sallow Gley

4.3 Discharge

In order to obtain more knowledge about the stream flow; and as mentioned before to determine the baseflow; the discharge of the stream flow was measured at different points in the stream. The first tests have been conducted by the Flow Tracker, since the measurements have not been sufficiently precise, two salt tracer tests were performed to measure the discharge of the stream. Moreover, a comparison between discharge measurements of an empty and a full system has been done. Therefore the test was conducted, once during a dry period in July, corresponding to an empty system and for discharge values of a full system another test was conducted in September after a rainy week and with high soil moisture conditions.

The measurements in July were conducted with dry conditions, i.e. without precipitation and a sufficiently low soil moisture. The results for the conducted salt tracer tests, are presented and discussed in this chapter:

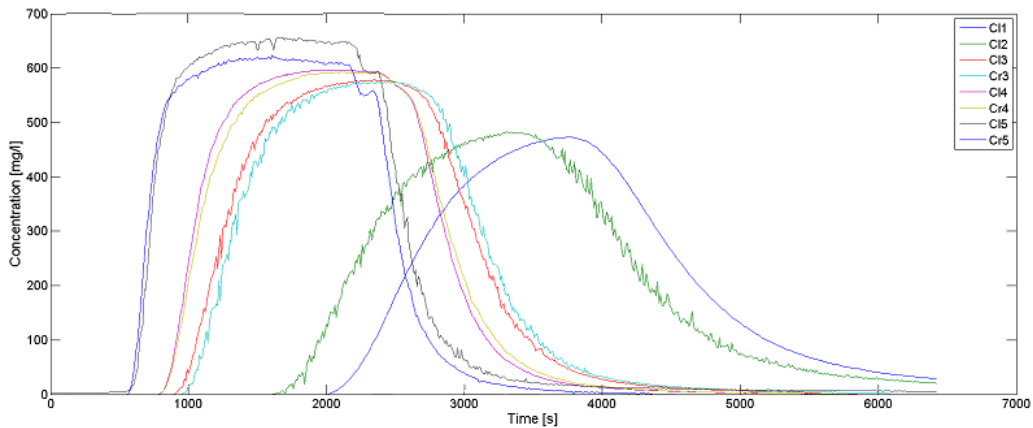


Figure 23: Salt tracer test in an empty system at the study area

For every measurement location two loggers were installed. One right and one left sided orthogonal to the main flow direction, as described in chapter 3.3. During the measurement two loggers stopped working due to low battery (the logger positioned right sided on location 1 and the logger positioned right sided on location 2). Hence, these data are missing on the plot (Fig. 23). Each logger represents one of the curves in figure 23. Location 5 was the closest to the injection point (Fig. 13), hence this was the first position to be reached by the salt tracer. The logger 5 on the right side detected the salt before the left sided logger. Due to the salt solution in the stream the electrical conductivity, the parameter obtained by the logger, raises. The logger positioned on the left reacts delayed on the higher conductivity, however shows a higher maximum value. Even the right-sided logger on location number 4 detected the higher conductivity due to the added salt solution faster than the left sided logger on position 4. Nevertheless both loggers measured the same values on the plateau. Also the right logger at location 3 was able to measure the increased conductivity before logger 3 on the left side. This circumstance is explained by the assumption, that the creek tends to flow faster on the right side. Both loggers on location 4 measured equivalent electrical conductivities and both loggers at location 3 obtained identical values, i.e. the salt solution has been completely mixed in the stream. The loggers on location 5 measured different plateau values; hence the solution was not yet properly mixed with the water, due to the short distance to the injection point. It can be seen in figure 23 that the measurements at location 1 and 2 do not show a proper plateau, i.e. only a short peak is recognizable. Hence, it is most likely that the dispersion of the salt solution was too high and thus the maximum concentration could be detected only during a short time period.

The plot of figure 24 shows that the discharge increases with increasing distance to the injection point. Accounting for the increasing discharge is an additionally water amount. Due to the fact, that during the measurements no overland flow existed and no tributary was detected, an interaction between the creek and the ground water is assumed in form of a baseflow.

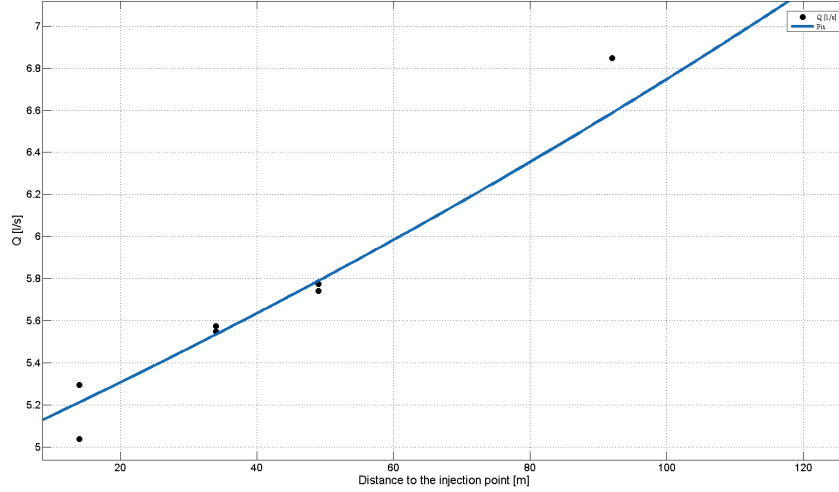


Figure 24: Discharge vs. distance to the injection point in an empty system

In order to determine the exact amount of discharge, the discharge was recalculated from the concentration as explained in chapter 3.3 with the corresponding equation (Eq. 10). This results in the values shown in table 5.

Table 5: Calculated discharge in an empty system (injection rate $q = 0.022 \text{ l/s}$, injection concentration $C1 = 150 \text{ g/l}$)

Measurement Position	$C2 \text{ [mg/l]}$	$Q \text{ [l/s]}$
M5R	623.25	5.30
M5L	654.81	5.04
M4R	594.65	5.55
M4L	591.84	5.58
M3R	574.59	5.74
M3L	571.31	5.78
M2L	481.85	6.85
M1L	470.15	7.02

Comparing the calculated Q-values of the different measurements one realizes that the discharge rises about 2 litres along the entire distance between the injection point and the end of the investigation area at measurement location 1. As mentioned before the stream is fed by water from the slope in form of baseflow. For detecting the differences in soil influence

on the stream by the baseflow, the loggers were located exactly on every soil border (Fig. 13).

The values of the gaining effect compared to the distance shows the additional running into the stream in each soil material.

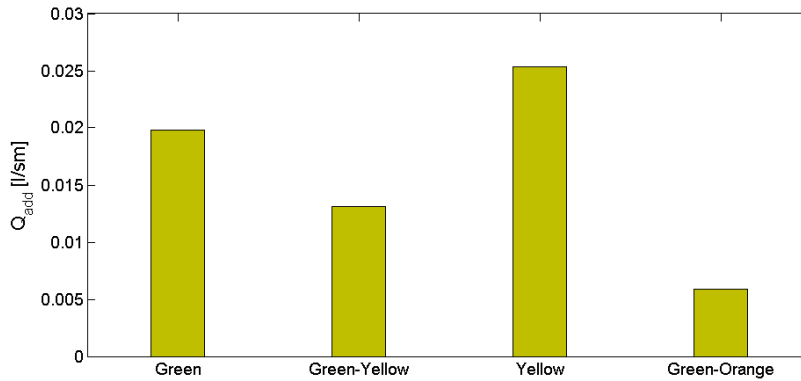


Figure 25: Calculated additional discharge per meter of every soil in an empty system green = extreme sallow gley; yellow = compact sallow gley; orange = acid sallow gley

Diagram (Fig. 25) represents the added water amount of the correlating soil in [l/m] and therefore shows that more water flows from the yellow soil into the creek than from the green soil. The yellow soil is defined by Kuhn (1994) as a compact sallow gley on the slip-off slope, whereby the green soil is defined as a compact, extreme sallow gley. In his study Germann (1981) detected a higher hydraulic conductivity in sallow gley than in extreme sallow gley. The fact that less water flows from the extreme sallow gley into the creek than from the sallow gley confirms Kuhn's studies.

From the green-orange part the deepest water amount flows into the creek, for two reasons. The orange soil is defined as an acid sallow gley and is influenced by a different geology than the other soils. Due to the fact it is abundant in gravel and poor in clayey components (Hottinger & Matter, 1970), it has a relatively high hydraulic conductivity and more water than from the other soils should flow into the creek. Nevertheless, a part of the creek bank in the orange area is concreted, due to a measurement station from the ETH, hence less water flows into the creek. The second reason for the low water amount flowing from the soil into the creek, is the short measured distance. It is assumed, that the water amount flowing from the soil into the creek is too low due to the short distance, that the loggers were not sensitive enough to recognize this gaining effect properly.

This case is confirmed by the fact, that the green-yellow mixed part should spend an average value of the green and yellow soil. However it is

much lower. Due to the fact, that this part is also relatively short, it is assumed, that the logger did not properly recognize the gaining effect as well. Hence, only the longer distances were observed and in summary, it can be stated that the yellow soil spends more water into the stream flow than the green soil. The question, which slope adds more water into the stream, can not be answered yet.

As mentioned before two salt tracer tests have been conducted, one in July and the other one in September. Based on a rainy week before the second salt tracer test, the soil moisture was greatly high and the system was filled up with water. Hence, different conditions than in July were given to conduct the salt tracer test. For comparing the values to the results of an empty system as in July, the loggers were located at the same location as during the measurements in July (Fig. 13). Nevertheless, in comparison to the first salt tracer test only one logger was installed per section. However during the measurements there was no precipitation, i.e. no overland flow existed. All the added water came in form of baseflow.

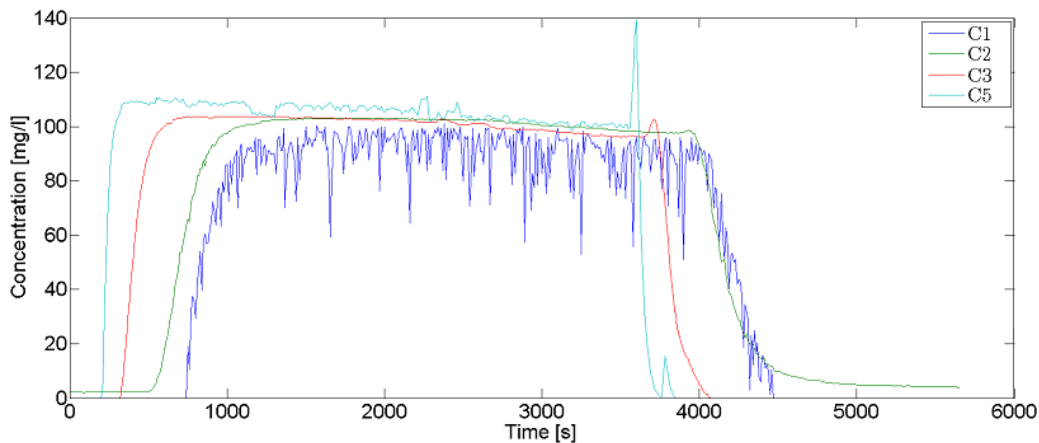


Figure 26: Salt tracer test in a full system at the study area

Figure 26 represents the measured concentration values during the salt tracer test in September. The logger on measurement location 4 was defect, hence the measurements on this position were ignored in this study.

Nevertheless, it is recognizable that the salt concentration achieved the logger on measurement location number 5 as first, then logger 3, before logger two detected a higher electric conductivity and at last logger 1 detected the salt concentration. Due to the larger water amount in the creek, which implemented a significant higher velocity of the discharge the concentration increases and decreases in comparison to the first salt tracer test steeper

and faster. The time differences between the starting points of the occurring plateaus are properly discernible. Logger 1 was located at the artificial measurement station from the ETH, there appears a little waterfall effect and thus air bubbles disturbed the measurements. However, the plateau is identifiable and the maximum concentration can be defined. Recalculated from the concentration to the discharge Q , table 6 shows that the discharge onto measurement location number 5 is about 30 l/s and location 1 measured about 33 l/s ; i.e. there is a gaining effect along the stream.

Table 6: Calculated discharge in a full system
(injection rate $q = 0.022\text{ l/s}$, injection concentration $C1 = 150\text{ g/l}$)

Measurement Position	$C2[\text{mg/l}]$	$Q[\text{l/s}]$
M5	109.03	30.27
M3	103.76	31.81
M2	102.68	32.14
M1	99.87	33.04

Figures 27 shows the relations of the water flow from different soils into the stream. In the full system the green soil spends large water amounts into the stream in comparison to the yellow soil. From the orange-green part a mean water amount flows into the stream. To sum up, one can say that from the green part, defined as a compact, extreme sallow gley, more water flows into the stream than from the yellow soil, defined as an acid, sallow gley. Due to the failed measurement on position 4, no “green-yellow soil“ appears in the results of salt tracer test in a full system.

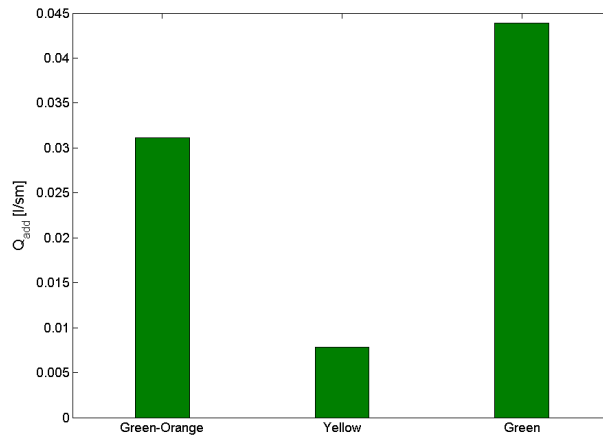


Figure 27: Calculated additional discharge per meter of every soil in a full system
 green = extreme sallow gley; yellow = compact sallow gley; orange = acid sallow gley

By comparing the soil parts of the empty system to the parts of the full system, it is found, that the relations are completely different. In an empty system the yellow soil spends more water into the stream than the green soil and in the full system the relation is inversed. Even the values of the orange-green part, are difficult to understand. However, by viewing the scale compared to the small values. It is uncertain if there is a possibility to measure as exact as possible of one liter per meter. The differences are smaller than 0.05 l/s . These differences are hard to discover and an inaccuracy of 0.01 l/m changes the diagram considerable.

Hence, comparing the influences of the different soils, was ignored, in order to concentrate on the complete gaining effect along the stream. This gaining effect was measured by the salt tracer test in an empty system, by a salt tracer test in a full system and additionally by a mini-flowmeter test. The results of the mini-flowmeter measurements are shown in figure 28. Also here, the results of these measurements show a gaining effect in a full system.

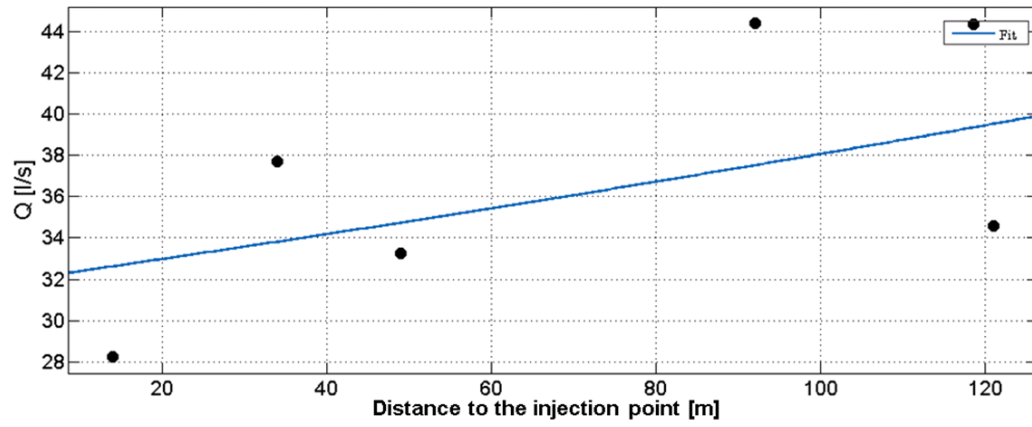


Figure 28: Discharge measured by the mini-flowmeter vs. the distance to the injection point

5 Conclusion and Outlook

For detecting the origins of floods of the Thur, the RECORD catchment project investigates its entire catchment. Floods have their origin in the catchment area of rivers and lakes thus it is important to have a detailed knowledge about the hydraulic processes affecting the water system in these areas. This thesis is integrated in the RECORD catchment project, performing analysis on the Rietholzbach, which is a tributary of the Thur.

The aim of this field study is to give an overview of the hydrological characterization of a part of the Rietholzbach area. The study slope is next to the Rietholzbach creek and is formed by a steep slope and a flat valley basin. The runoff components precipitation, infiltration, overland flow, base-flow and stream flow were investigated and analyzed. For the generation of flood events, especially the overland flow is of importance due to the fact, that this discharge component is the fastest process during discharge generation.

The infiltration behaviour of the slope changes decreasing top down and never reaches saturated infiltration values higher than $1\text{ cm}/\text{min}$. The infiltration rate is initially high, then decreases with time and becomes finally constant. The time until the constant rate is reached, is mainly affected by the initial degree of saturation of the soil. Thus it can be concluded that the initial saturation has major influence on the occurrence of overland flow, since it is only generated once the soil is fully saturated. Hence, the higher the initial saturation of the soil, the faster the appearance of overland flow. As soon as the precipitation rate is higher than the infiltration rate overland flow will occur. Based on the conducted investigations, the overland flow could be calculated. Hence, an overland flow in saturated conditions is expected, when the precipitation rate increases above $0.23\text{ cm}/\text{min}$, respectively $139\text{ mm}/\text{h}$. This is likely to happen in the lower part of the investigation area, whereas in the upper part, more steeper, it is almost impossible to reach the critical infiltration rate. For the investigation of the hydraulic conductivity of the subsurface several slug-out tests were conducted. Here, the highest hydraulic conductivity of the subsurface was measured on top of the investigation area with a value of $1.02 \times 10^{-4}\text{ m}/\text{s}$, the lowest value was measured next to the creek $2.30 \times 10^{-6}\text{ m}/\text{s}$. This can be explained by the fact that small clay particles are leached in the slope and transported down towards the valley basin. These particles are able to fill larger pores and bind the water due to the high cohesion coefficient of the clay. Hence, the hydraulic conductivity becomes minimal in the area around the creek. Thus it can be assumed that

the groundwater flow is faster in steep regions, i.e. the slope, compared to the almost horizontal valley basin.

The conducted salt tracer test for determining the discharge along the investigated Rietholzbach section showed in an empty as well as in a full system a gaining effect of the stream. This finding was confirmed by a mini-flowmeter test which was conducted after a period of rain, i.e. in a full system. Due to the fact that during the measurements no overland flow was observed and no tributary to the stream was detected, it can be concluded that an interaction between the stream flow and the ground water in form of baseflow can be assumed. In an empty system the baseflow occurs and adds 1.8 liter water into the stream along the study slope. In a full system 2.8 liter of groundwater in the investigated area are flowing into the stream. The investigated slope of the pre-alpine area of the Rietholzbach spends water into the stream flow directly by the overland flow in saturated conditions during a precipitation event and indirectly in form of baseflow. The discharge of the Rietholzbach increases by passing through the investigated part of the Rietholzbach catchment due to the permanent inflow of ground water, in an empty and full system.

Since the values of the double-ring infiltrometer measurements and the slug-out tests correlate well to the soil map of Kuhn (1980), the map may be used for further investigations regarding hydraulic characterization of the soil in this area, thus additional field measurements can be avoided.

Since the Thur river influences the groundwater, knowledge about the components affecting the discharge is essential. The propinquity to the stream flow has a low hydraulic conductivity, i.e. the interaction between groundwater and stream is slow. This investigation also shows, that during dry as well as during wet periods only the region next to the stream affects the discharge of the stream. Further studies will examine the response time of the groundwater by a tracer test in the slope. This test is necessary to determine the reservoir effect on the percolation, interflow and the baseflow in this area. Moreover the hydraulic characterization of the opposite slope is relevant to understand the runoff components of the study slope as well as of the entire catchment area. In order to perform a detailed modeling of the study area, further investigations on parameters like influence of the steepness on the groundwater flow and the Horton overland flow, which appears in the unsaturated soil, would be helpful.

6 Summary

Water is life – and sometimes destruction and death in form of floods. These may occur regularly in nature and endanger humans and the environment. For this reason the research of floods and its origin is compelling. This thesis is integrated in the RECORD catchment project of the Eawag and is located on the Rietholzbach, which is a tributary of the Thur river. The aim of this study is to give an overview of the hydraulic characteristic of a part of the Rietholzbach area.

The area investigated in this study is located in the middle of the Rietholzbach catchment area in the pre-alpine parts of Northeastern Switzerland. More precise it is the area next to the ETH measurement site “Büel“ in Kirchberg. The geology of the catchment area from the Rietholzbach is characterized by tertiary deposits of the Upper Freshwater Molasse, which belong to the sedimentation of the almost horizontal stratified Hörnli-Fan Deposits “Hörnlschuttfächer“. Two different main soil types occur in the study area: brown earth and gley.

In order to determine the infiltration rate in the study area described before double-ring infiltration measurements were conducted, since this is a well-established method. It consists of two concentric open cylinders driven in the ground. Testing the infiltration rate works by filling the rings partially with water and periodical measuring the water level while the water in the rings infiltrate into the soil. The measured infiltration rates correlates to the characteristic of the soils defined by the soil map of Kuhn (1980). The highest measured infiltration rate in the investigation area is 1.5cm/min. Due to the fact that only the infiltration rate in saturated soils are interesting for this study, just the end-values are considered. Thus the highest value found is 1cm/min of double-ring infiltrometer measurement on top of the slope and the lowest infiltration rate detected was 0 cm/min at the lowest part of the investigation area, next to the stream. It is also possible to recognize that the infiltration rate does not only change by the slope height. The right-sided measured values show, that there is a different soil. The geology map can explain this issue. A wallmorain reaches into the right side of the investigation area, which implements a different soil, than the residual area, which is formed by a ground moraine. Due to the fact that the wallmorain is formed with less clayey elements than the ground morain, the soil is less gleyey and thus shows a higher hydrological conductivity respectively a higher infiltration rate.

In order to determine the baseflow it is of major importance to have detailed knowledge about the aquifer characteristic. A slug test is one of the

aquifer test methods commonly used to investigate aquifer parameters (Yeh & Yang, 2006). The principle of slug tests is based on an abrupt artificially created change of a hydrological gradient between a test-well and the groundwater level. The water-level changes due to a falling slug-body pushing the water into the aquifer (slug-in test) or due to a slug-body displacing parts of the water (slug-out test). Characterizing the aquifer is the duration during which the water level returns to the still-water level measured by a logger. As by the double-ring infiltrometer measurements, so the results of the slug-out tests were interpolated by the software ArcMap (ESRI) and the method "Kriging". There is an exponential correlation between the distance to the stream and hydraulic conductivity. As bigger the distance to the stream, the higher is the hydraulic conductivity. This circumstance can be explained by the fact, that the hydraulic conductivity depends on the soil character. From the soil map of Kuhn (1980) it is known, that the soil changes by the distance to the stream. It becomes dryer and less gleyey, hence the soil's hydraulic conductivity increases with the distance. Thus, the correlation between distance to the stream and the hydraulic conductivity values is given.

The first discharge measurements have been conducted by a Flow Tracker, since the measurements have not been sufficiently precise, also a salt tracer test was performed to measure the discharge of the stream. At an input location, a precisely defined amount of a salt is fed into the water. The concentration of the diluted tracer in the flowing water is measured by a logger on a cross section downstream of the flow. The distance between input and measuring point ensures the complete mixing of the salt tracer with the stream water. The observed concentration of the measuring point determines the dilution. Since the input amount of salt is known, it is possible to calculate the stream flow using the dilution value. The measurements show that the salt concentration decreases with increasing distance to the pumping station. Accounting for the decreasing concentration is an additionally water amount. Due to the fact, that during the measurements no overland flow existed and no tributary was detected, an interaction between the creek and the ground water is assumed in form of a baseflow.

The investigated slope of the pre-alpine area of the Rietholzbach spends water into the stream flow, directly by the overland flow during a precipitation event and indirectly in form of baseflow. The discharge of the Rietholzbach increases by passing through this area in an empty as well as in a full system, due to the permanent inflow from the ground water.

Further researches in this area are essential for the understanding of the entire runoff components in this area. In order determine the reservoir effect a salt tracer test is necessary to investigate the percolation, interflow and the baseflow in this area.

List of Figures

1	Location of the Thur catchment, the Thur valley aquifer and different test sites at Neunforn (partly restored) and Widen (channelized) as well as the Rietholzbach area in NE Switzerland (Schneider et al., 2011)	6
2	Location of the measurement site Büel in the Rietholzbach catchment (left) and the study area in comparison to the PhD-study area (Seneviratne, 2012)	7
3	Geology Map of the investigation area (after Hottinger and Matter, 1970)	9
4	Soil map of the investigation area (after Kuhn, 1980)	10
5	Climate diagram based on data of the time period 1976-2007 (IACETH, 2013)	11
6	Components of Runoff	12
7	Example of a double-ring infiltrometer construction as used in this study	16
8	Positions of the conducted double-ring infiltrometer measurements	17
9	Positions of the slug-out test wells	20
10	A schematic view of the well constructions (AQTESOLV, 2013)	21
11	Example of an AQTESOLV Diagram	24
12	Schematic figure of a Flow Tracker (Quantum Hydrometrie, 2012)	25
13	Measurement points (M) of the discharge measurements (Kuhn, 1980)	27
14	Mini-Flowmeter (MiniAir2 Schiltknecht)	29
15	Double-Ring Infiltration Measurement 2	31
16	Double-Ring Infiltration Measurement 10	32
17	Double-Ring Infiltration Measurement 9	33
18	Infiltration rate over time of all conducted double-ring infiltrometer measurements	34
19	Interpolation Map of the Double-Ring Infiltration Measurements, Base map (Kuhn, 1980)	35
20	Schematic view of well number 6 with the negative b value	38
21	Hydraulic conductivity vs. the distance to the stream	39
22	Interpolation Map of the Slug-out Tests Base map (Kuhn, 1980)	40
23	Salt tracer test in an empty system at the study area	41
24	Discharge vs. distance to the injection point in an empty system	43

25	Calculated additional discharge per meter of every soil in an empty system green = extreme sallow gley; yellow = compact sallow gley; orange = acid sallow gley	44
26	Salt tracer test in a full system at the study area	45
27	Calculated additional discharge per meter of every soil in a full system green = extreme sallow gley; yellow = compact sallow gley; orange = acid sallow gley	47
28	Discharge measured by the mini-flowmeter vs. the distance to the injection point	48

List of Tables

1	Potential infiltration rate in the study area	36
2	Well 1-5	37
3	Well 6-8	38
4	DIN-Classification (DIN 18130, 1998) vs. Kuhn-Classification (Kuhn,1980)	41
5	Calculated discharge in an empty system (injection rate $q =$ 0.022 l/s , injection concentration $C1 = 150\text{ g/l}$)	43
6	Calculated discharge in a full system (injection rate $q = 0.022\text{ l/s}$, injection concentration $C1 = 150\text{ g/l}$)	46

References

- AQTESOLV (2013). AQTESOLV: Product - unpublished.
- ASTM (2009). ASTM D3385–Standard Test Method for Infiltration Rate of Soils in Field Using Double-Ring Infiltrometer. ASTM International.
- BAFU (2013). Hydrologische Grundlagen und Daten, Stationsdaten, Thur - Andelfingen, 2044 - unpublished.
- Balderer, W. (1979). Die Obere Süsswassermolasse als hydrogeologisches Gesamtsystem. Bull. Centre d'Hydrogeologie de Neuchatel.
- Bouwer, H. (1989). The Bouwer and Rice Slug Test—an Update. *Ground Water*, 27(3), 304–309.
- Bouwer, H. & Rice, R. (1994). A Slug Test Method for Determining Hydraulic Conductivity of Unconfined Aquifers with Completely or Partially Penetrating Wells. *Water Resources Research*, 12(3), 423–428.
- Brady, N. & Weil, R. (1999). The Nature and Properties of Soils. 9th Edition - Macmillan Publishing Company, New York.
- Butler, J.-J. J. (1997). *The Design, Performance, and Analysis of Slug Tests*. CRC Press.
- CCES (2013). RECORD Catchment: Project Summary - unpublished.
- DIN (1998). Deutsches Institut für Normung 18130, Blatt 9.
- DIN (2007). Deutsches Institut für Normung 19682, Blatt 7.
- Dutter, R. (1985). *Geostatistik: Mathematische Methoden in der Technik - 2*. Stuttgart: B.G. Teubner.
- Eckhardt, K. (2008). A comparison of baseflow indices, which were calculated with seven different baseflow separation methods. *Journal of Hydrology*, 352(1–2), 168 – 173.
- Fetter, C. (1994). Applied Hydrogeology. 3–Macmillan College Publishing Company, New York.
- Germann, P. (1981). *Untersuchungen über den Bodenwassergehalt im hydrologischen Einzugsgebiet Rietholzbach*. Diploma Thesis, ETH Zürich.

- Green, W. & Ampt, G. (1911). Studies in Soil Physics - the Flow of Air and Water through Soils. *Agricultural Science*, 4, 1–24.
- Grutz, J., Badertscher, S., Milzow, C., Moser, U., Schroff, K., Stoeckli, R., Völksch, I., & Zingg, M. (2006). Analysis of the time series of meteorological and hydrological measurements in the Rietholzbach research catchment between 1976 and 2005 with special consideration of the dry summer 2003. Institut für Atmosphäre und Klima der ETH Zürich.
- Hottinger, L. & Matter, A. (1970). Erläuterungen zu Blatt 1093 Hörnli. Schweiz. Geol. Kommission, Zürich.
- IACETH (2013). Climate diagram based on data of the time period 1976–2007 - unpublished.
- Jardani, A., Revil, A., & Dupont, J. (2013). Stochastic joint inversion of hydrogeophysical data for salt tracer test monitoring and hydraulic conductivity imaging. *Advances in Water Resources*, 52(0), 62 – 77.
- Koskelo, A. I., Fisher, T. R., Utz, R. M., & Jordan, T. E. (2012). A new precipitation-based method of baseflow separation and event identification for small watersheds. *Journal of Hydrology*, 450–451(0), 267 – 278.
- Kuhn, H. (1994). Bodenkartierung HYDREX. Versuchsanstalt für Wasserbau, Hydrologie und Glaziologie der ETH Zürich.
- Leibundgut, C. & Seibert, J. (2011). Tracer Hydrology. *Treatise on Water – Science Academic Press*, (pp. 215–236).
- McElwee, C. (2002). Improving the Analysis of Slug Tests. *Journal of Hydrology*, 269, 122–133.
- Philip, J. R. (1957). The theory of Infiltration - Sorptivity and algebraic Infiltration Equations. *Soil Science*, 84, 257–264.
- Scheffer, F. & Schachtschabel, P. (2010). *Lehrbuch der Bodenkunde*. Spektrum, 16. auflage edition.
- Schneider, P., Vogt, T., Schirmer, M., Doetsch, J., Linde, N., Pasquale, N., Perona, P., & Cirpka, O. A. (2011). Towards improved instrumentation for assessing river-groundwater interactions in a restored river corridor. *Hydrology and Earth System Sciences*, 15(8), 2531–2549.

- Seneviratne, S. I., Lehner, I., Gurtz, J., Teuling, A. J., Lang, H., Moser, U., Grebner, D., Menzel, L., Schroff, K., Vitvar, T., & Zappa, M. (2012). Swiss prealpine rietholzbach research catchment and lysimeter: 32 year time series and 2003 drought event. *Water Resources Research*, 48(6).
- Sidiras, N. & Roth, C. (1987). Infiltration measurements with double-ring infiltrometers and a rainfall simulator under different surface conditions on an oxisol. *Soil and Tillage Research*, 9(2), 161 – 168.
- Weiler, M. & Naef, F. (2003). An Experimental Tracer Study of the Role of Macropores in Infiltration in Grassland Soils. *Hydrological Processes*, 17, 477–493.
- Yeh, H.-D. & Yang, S.-Y. (2006). A Novel Analytical Solution for a Slug Test Conducted in a Well with a Finite-Thickness Skin. *Advances in Water Resources*, 29(10), 479–489.
- Youngs, E. (1972). Two- and Three-Dimensional Infiltration: Seepage from Irrigation Channels and Infiltration Rings. *Journal of Hydrology*, 15(4), 301–315.
- Ziegler, A., Sutherland, R., & Giambelluca, T. (2001). Acceleration of horton overland flow and erosion by footpaths in an upland agricultural watershed in northern thailand. *Geomorphology*, 41(4), 249 – 262.
- Zuidema, P. (1985). *Hydraulik der Abflussbildung während Starkniederschlägen – eine Untersuchung mit Hilfe numerischer Modelle unter Verwendung plausibler Bodenkennwerte*. Diploma Thesis, ETH Zürich.

Personal Declaration

I hereby declare that the submitted thesis is the result of my own, independent, work. All external sources are explicitly acknowledged in the thesis.

A handwritten signature in black ink, appearing to be 'C. J.', is centered on the page.